PTEP

Prog. Theor. Exp. Phys. **2015**, 033B04 (23 pages)
DOI: 10.1093/ptep/ptv017

Imprints of CP-violation asymmetries in rare $\Lambda_b \to \Lambda \ell^+ \ell^-$ decay in a family non-universal Z' model

M. Ali Paracha[1,2,*], Ishtiaq Ahmed[1,4,*], and M. Jamil Aslam[3,*]

[1]*Laboratório de Física Teórica e Computacional, Universidade Cruzeiro do Sul, 01506-000 São Paulo, Brazil*
[2]*Department of Physics, School of Natural Sciences, National University of Science and Technology, Islamabad 44000, Pakistan*
[3]*Department of Physics, Quaid-i-Azam University, Islamabad 45320, Pakistan*
[4]*National Centre for Physics, Quaid-i-Azam University Campus, Islamabad 45320, Pakistan*
*E-mail: paracha@phys.qau.edu.pk, ishitaq@ncp.edu.pk, jamil@phys.qau.edu.pk

Received October 28, 2014; Revised January 21, 2015; Accepted January 21, 2015; Published March 16, 2015

We investigate the exclusive rare baryonic $\Lambda_b \to \Lambda \ell^+ \ell^-$ decay in a family non-universal Z' model, which is one of the natural extensions of the Standard Model. Using transition form factors, calculated in the framework of light-cone QCD sum rules, we analyze the effects of polarized and unpolarized CP-violation asymmetries on the above-mentioned semileptonic decays of the Λ_b baryon. Our results indicate that the values of unpolarized and polarized CP-violation asymmetries are considerable in both the $\Lambda_b \to \Lambda \mu^+ \mu^-$ and $\Lambda_b \to \Lambda \tau^+ \tau^-$ channels, and hence they give a clear indication of new physics arising from the neutral Z' gauge boson. It is hoped that the measurements of these CP-violating asymmetries will not only help us to find hints of new physics, but also provide a tool to determine the precise values of the parameters of the Z' gauge boson.

Subject Index B51, B52, B56, B57

1. Introduction

Despite the discovery of the last missing chunk of the Standard Model (SM), the Higgs boson, and its phenomenological success, there are hints that paths to new physics (NP) are open. The flavor sector is one of the key areas that occurs in these paths. The joint efforts at hadron colliders and B factories have provided us with data of unprecedented precision in this sector; these data are not sensitive to small effects in theoretical calculations that are essential in comparison with the experimental measurements, and will enable us to see if there are any hints of NP.

There are two approaches that are mainly considered to investigate physics beyond the Standard Model. The first approach is the direct search for new particles, i.e. where the particles corresponding to different NP models are produced: the most attractive in this class are different supersymmetric models, where the energy of the colliders is raised. The second approach is the indirect search, i.e., to increase the experimental precision on the data of different SM processes where NP effects can manifest themselves. The focus of the two major detectors, ATLAS and CMS, at the Large Hadron Collider (LHC) at CERN is to detect the possible new particles produced at sufficiently large energy. However, in indirect searches, flavor physics plays an important role in investigating physics in and

Funded by SCOAP[3]

beyond the SM, and the experiments that represent the precision frontier are LHCb at LHC and Belle II at Super-KEKB. It is possible that other planned super-B factories will join this arena in the future.

In the precision approach, the processes that are suitable to investigate physics in and beyond the SM are rare decays, particularly the decays that are described by $b \to s(d)$ transitions. The attractive features of such decays are that they are not allowed at tree level in the SM and occur only at loop level [1]. Therefore, these decays serve as excellent candidates to chalk out the status of new physics beyond the SM. In the mesonic sector, rare decays of B mesons have been widely studied both theoretically and experimentally in detail [2–5].

It is well known that the predictions of the SM results are in good agreement with the current experimental data; however, there are still some unanswered questions in this elegant model, e.g., CP violation, the hierarchy puzzle, neutrino oscillations, to name a few. To answer these questions, a large number of NP models, such as extra-dimension models, different versions of supersymmetric models, etc., exist in the literature; extensive studies on the exclusive semileptonic decays of B mesons and baryonic Λ_b have also already been done on these models [6–16].

In grand unified theories such as $SU(5)$ or string-inspired E_6 models [17–21], one of the most relevant is the Z' scenarios, which include the family non-universal Z' [22,23] and leptophobic Z' models [24,25]. Experimental searches for an extra Z' boson is an important task of the Tevatron [26] and LHC [27,28] experiments. On the other hand, obtaining the constraints on the Z' gauge boson couplings through low-energy processes is crucial and complementary to direct searches $Z' \to e^+e^-$ at Tevatron [29]. The most interesting thing about the family non-universal Z' model is the new CP-violating phase, which has large effects on various flavor-changing neutral-current (FCNC) processes [23,30,31], such as $B_s - \bar{B}_s$ mixing [32–47] and rare hadronic B meson decays [48–67].

In the baryonic sector, exclusive $\Lambda_b \to \Lambda\ell^+\ell^-(\ell = \mu, \tau)$ decays at quark level are described by a $b \to s\ell^+\ell^-$ transition. The main difference between these and other mesonic decays is that they can give information about the helicity structure of the effective Hamiltonian for the FCNC $b \to s$ process in the SM and beyond [68]. On the experimental side, the first observation of rare baryonic $\Lambda_b \to \Lambda\mu^+\mu^-$ decay has been made by the CDF Collaboration [69], and recently this decay has also been studied by the LHCb Collaboration [70]. These experimental investigations provide a strong motivation to perform analyses of different physical observables such as branching ratio, forward–backward asymmetry, single and double lepton polarization asymmetries, and CP-violation asymmetry in these decay modes. It is to be hoped that such studies are useful to distinguish various extensions of the SM.

In the present work, we analyze the effects of polarized and unpolarized CP-violation asymmetries on $\Lambda_b \to \Lambda\ell^+\ell^-$ decay in the family non-universal Z' model [23]. It is important to emphasize here that the matrix elements for $b \to s$ transitions are proportional to three quark-coupling matrix elements usually called Cabibbo–Kobayashi–Maskawa (CKM) matrix elements, $V_{tb}V_{ts}^*$, $V_{cb}V_{cs}^*$, and $V_{ub}V_{us}^*$. However, due to the unitarity condition, and neglecting the matrix elements $V_{ub}V_{us}^*$ in comparison with $V_{tb}V_{ts}^*$ and $V_{cb}V_{cs}^*$, the CP asymmetry is highly suppressed in the SM for the decays probed through FCNC transitions. Therefore, the measurements of CP-violating asymmetries in $b \to s$ decays play an important role in finding the imprints of the Z' model.

The structure of the paper is as follows. In Sect. 2, we develop a theoretical toolbox in which we present the effective Hamiltonian for the decay $b \to s\ell^+\ell^-$. In the same section, we present the transition matrix element for the $\Lambda_b \to \Lambda\ell^+\ell^-$ decay, and the expressions for unpolarized and

polarized CP violation for the said decay in the family non-universal Z' model. In Sect. 3, we discuss the numerical results of the above-mentioned physical observables. Concluding remarks are also presented in the same section.

2. Theoretical toolbox

At quark level, the decay $\Lambda_b \to \Lambda \ell^+ \ell^-$ ($\ell = \mu, \tau$) is governed by the transition $b \to s\ell^+\ell^-$; the effective Hamiltonian for such decays at the $O(m_b)$ scale can be written as

$$H_{\rm eff} = -\frac{4G_{\rm F}}{\sqrt{2}} V_{tb} V_{ts}^* \sum_{i=1}^{10} C_i(\mu) O_i(\mu), \tag{1}$$

where $G_{\rm F}$ is the Fermi coupling constant and V_{ij} are the matrix elements of the CKM matrix. In Eq. (1), $O_i(\mu)$ are the local quark operators and $C_i(\mu)$ are the corresponding Wilson coefficients at energy scale μ. The explicit expressions for the Wilson coefficients at next-to-leading logarithm order and next-to-next leading logarithm are given in Refs. [71–80]. The operators responsible for such decays are O_7, O_9, and O_{10}, which are summarized as [12]:

$$O_7 = \frac{e^2}{16\pi^2} m_b \big(\bar{s}\sigma_{\mu\nu} R b\big) F^{\mu\nu} \tag{2}$$

$$O_9 = \frac{e^2}{16\pi^2} \big(\bar{s}\gamma_\mu L b\big)\, \bar{\ell}\gamma^\mu \ell \tag{3}$$

$$O_{10} = \frac{e^2}{16\pi^2} \big(\bar{s}\gamma_\mu L b\big)\, \bar{\ell}\gamma^\mu \gamma^5 \ell.$$

In terms of the effective Hamiltonian given in Eq. (1), the quark level amplitude for the said decay in the SM can be written as

$$\mathcal{M}^{\rm SM}\big(b \to s\ell^+\ell^-\big) = -\frac{G_{\rm F}\alpha}{\sqrt{2}\pi} V_{tb} V_{ts}^* \Big\{ C_9^{\rm eff} \big(\bar{s}\gamma_\mu L b\big)\big(\bar{\ell}\gamma^\mu \ell\big) + C_{10}^{\rm SM} \big(\bar{s}\gamma_\mu L b\big)\big(\bar{\ell}\gamma^\mu \gamma_5 \ell\big) - 2m_b C_7^{\rm eff} \left(\bar{s} i\sigma_{\mu\nu} \frac{q^\nu}{q^2} R b\right)\left(\bar{\ell}\gamma^\mu \ell\right)\Big\}, \tag{4}$$

where q^2 is the square of the momentum transfer and α is the fine structure constant. Also, in operator O_7 the mass of the strange quark (m_s) is ignored compared to m_b.

A family non-universal Z' boson could be derived naturally in many extensions of the SM; the most economical way to get it is to include an additional $U'(1)$ gauge symmetry. This model has been formulated in detail by Langacker and Plümacher [23]. In a family non-universal Z' model, the FCNC transitions $b \to s\ell^+\ell^-$ could be induced at tree level because of the non-diagonal chiral-coupling matrix. Assuming that the couplings of right-handed quark flavors with the Z' boson are diagonal and ignoring Z–Z' mixing, the effective Hamiltonian corresponding to the Z' part for the $b \to s\ell^+\ell^-$ transition can be written as [81–89]

$$\mathcal{H}_{\rm eff}^{Z'}\big(b \to s\ell^+\ell^-\big) = -\frac{2G_{\rm F}}{\sqrt{2}} V_{tb} V_{ts}^* \left[\frac{B_{sb} S_{\ell\ell}^L}{V_{tb} V_{ts}^*} \big(\bar{s}b\big)_{V-A} \big(\bar{\ell}\ell\big)_{V-A} + \frac{B_{sb} S_{\ell\ell}^R}{V_{tb} V_{ts}^*} \big(\bar{s}b\big)_{V-A} \big(\bar{\ell}\ell\big)_{V+A}\right]. \tag{5}$$

Here, $S^L_{\ell\ell}$ and $S^R_{\ell\ell}$ represent the couplings of the Z' boson with the left- and right-handed leptons, respectively, $B_{sb} = |\mathcal{B}_{sb}|e^{-i\phi_{sb}}$ corresponds to the off-diagonal left-handed coupling of quarks with the new Z' boson, and ϕ_{sb} corresponds to a new weak phase.

In a more compact form, Eq. (5) becomes

$$\mathcal{H}^{Z'}_{\rm eff}(b \to s\ell^+\ell^-) = -\frac{4G_{\rm F}}{\sqrt{2}} V_{tb}V^*_{ts}\left[\Lambda_{sb}C^{Z'}_9 O_9 + \Lambda_{sb}C^{Z'}_{10}O_{10}\right], \tag{6}$$

where

$$\Lambda_{sb} = \frac{4\pi e^{-i\phi_{sb}}}{\alpha_{\rm EM}V_{tb}V^*_{ts}} \tag{7}$$

$$C^{Z'}_9 = |\mathcal{B}_{sb}|S_{LL}; \quad C^{Z'}_{10} = |\mathcal{B}_{sb}|D_{LL}, \tag{8}$$

and

$$\begin{aligned} S_{LL} &= S^L_{\ell\ell} + S^R_{\ell\ell}, \\ D_{LL} &= S^L_{\ell\ell} - S^R_{\ell\ell}. \end{aligned} \tag{9}$$

The most economical feature of the family non-universal Z' model is that operator basis remains the same as in the SM and the only modification occurs in the Wilson coefficients C_9 and C_{10}, while the Wilson coefficient $C^{\rm eff}_7$ remains unchanged.

The total amplitude for the decay $\Lambda_b \to \Lambda\ell^+\ell^-$ is the sum of the SM and Z' contributions, i.e.,

$$\begin{aligned} \mathcal{M}^{\rm tot}(\Lambda_b \to \Lambda\ell^+\ell^-) = -\frac{G_{\rm F}\alpha}{2\sqrt{2}\pi}V_{tb}V^*_{ts}\Big[&\langle\Lambda(k)|\bar{s}\gamma_\mu(1-\gamma_5)b|\Lambda_b(p)\rangle\{C^{\rm tot}_9(\bar{\ell}\gamma^\mu\ell) \\ &+ C^{\rm tot}_{10}(\bar{\ell}\gamma^\mu\gamma^5\ell)\} - \frac{2m_b}{q^2}C^{\rm eff}_7\langle\Lambda(k)|\bar{s}i\sigma_{\mu\nu}q^\nu(1+\gamma^5)b|\Lambda_b(p)\rangle\bar{\ell}\gamma^\mu\ell\Big], \end{aligned} \tag{10}$$

where $C^{\rm tot}_9 = C^{\rm eff}_9 + \Lambda_{sb}C^{Z'}_9$ and $C^{\rm tot}_{10} = C^{\rm SM}_{10} + \Lambda_{sb}C^{Z'}_{10}$.

The matrix elements for the decay $\Lambda_b \to \Lambda\ell^+\ell^-$ can be straightforwardly parameterized in terms of the form factors as follows [90]:

$$\begin{aligned} \langle\Lambda(k)|\bar{s}\gamma_\mu(1-\gamma_5)b|\Lambda_b(p)\rangle = \bar{u}_{\Lambda(k)}\Big[&f_1(q^2)\gamma_\mu + i\sigma_{\mu\nu}q^\nu f_2(q^2) + q^\mu f_3(q^2) - \gamma_\mu\gamma_5 g_1(q^2) \\ &- i\sigma_{\mu\nu}q^\nu\gamma_5 g_2(q^2) - q^\mu\gamma_5 g_3(q^2)\Big]u_{\Lambda_b(p)}, \end{aligned} \tag{11}$$

$$\begin{aligned} \langle\Lambda(k)|\bar{s}i\sigma^{\mu\nu}q^\nu(1+\gamma_5)b|\Lambda_b(p)\rangle = \bar{u}_{\Lambda(k)}\Big[&f^T_1(q^2)\gamma_\mu + i\sigma_{\mu\nu}q^\nu f^T_2(q^2) + q^\mu f^T_3(q^2) \\ &+ \gamma_\mu\gamma_5 g^T_1(q^2) + i\sigma_{\mu\nu}q^\nu\gamma_5 g^T_2(q^2) + q^\mu\gamma_5 g^T_3(q^2)\Big]u_{\Lambda_b(p)}, \end{aligned} \tag{12}$$

where f_i, g_i and f^T_i, g^T_i are the transition form factors for the decay $\Lambda_b \to \Lambda$.

By using the matrix elements that are parameterized in terms of transition form factors (c.f. Eqs. (11) and (12)), the decay amplitude for $\Lambda_b \to \Lambda\ell^+\ell^-$ decay can be written as

$$\mathcal{M}^{\rm tot}(\Lambda_b \to \Lambda\ell^+\ell^-) = \frac{G_{\rm F}\alpha_{\rm EM}}{2\sqrt{2}\pi}V_{tb}V^*_{ts}\left[\bar{u}_{\Lambda(k)}\left\{\tau^1_\mu(\bar{\ell}\gamma^\mu\ell) + \tau^2_\mu(\bar{\ell}\gamma^\mu\gamma^5\ell)\right\}\right]u_{\Lambda_b(p)}\Big]. \tag{13}$$

The hadronic functions τ_μ^1 and τ_μ^2 are given by

$$\tau_\mu^1 = A(q^2)\gamma_\mu + iB(q^2)\sigma_{\mu\nu}q^\nu + C(q^2)q_\mu - D(q^2)\gamma_\mu\gamma_5 - iE(q^2)\sigma_{\mu\nu}q^\nu\gamma^5 - F(q^2)q_\mu\gamma^5 \quad (14)$$

$$\tau_\mu^2 = G(q^2)\gamma_\mu + iH(q^2)\sigma_{\mu\nu}q^\nu + I(q^2)q_\mu - J(q^2)\gamma_\mu\gamma_5 - iK(q^2)\sigma_{\mu\nu}q^\nu\gamma^5 - L(q^2)q_\mu\gamma^5. \quad (15)$$

The auxiliary functions from $A(q^2)$ to $L(q^2)$ given in Eqs. (14) and (15) contains both short- and long-distance effects, which are encapsulated in terms of Wilson coefficients and form factors. The explicit form of these functions can be written as follows:

$$\begin{aligned}
A(q^2) &= C_9^{\rm tot} f_1(q^2) - \frac{2m_b}{q^2} C_7^{\rm eff} f_1^T(q^2) \\
B(q^2) &= C_9^{\rm tot} f_2(q^2) - \frac{2m_b}{q^2} C_7^{\rm eff} f_2^T(q^2) \\
C(q^2) &= C_9^{\rm tot} f_3(q^2) - \frac{2m_b}{q^2} C_7^{\rm eff} f_3^T(q^2) \\
D(q^2) &= C_9^{\rm tot} g_1(q^2) - \frac{2m_b}{q^2} C_7^{\rm eff} g_1^T(q^2) \\
E(q^2) &= C_9^{\rm tot} g_2(q^2) - \frac{2m_b}{q^2} C_7^{\rm eff} g_2^T(q^2) \\
F(q^2) &= C_9^{\rm tot} g_3(q^2) - \frac{2m_b}{q^2} C_7^{\rm eff} g_3^T(q^2) \\
G(q^2) &= C_{10}^{\rm tot} f_1(q^2) \\
H(q^2) &= C_{10}^{\rm tot} f_2(q^2) \\
I(q^2) &= C_{10}^{\rm tot} f_3(q^2) \\
J(q^2) &= C_{10}^{\rm tot} g_1(q^2) \\
K(q^2) &= C_{10}^{\rm tot} g_2(q^2) \\
L(q^2) &= C_{10}^{\rm tot} g_3(q^2).
\end{aligned} \quad (16)$$

The matrix element for the decay $\Lambda_b \to \Lambda\ell^+\ell^-$ given in Eq. (13) is useful to calculate the physical observables. The formula for the double differential decay rate can be written as

$$\frac{d^2\Gamma(\Lambda_b \to \Lambda\ell^+\ell^-)}{d\cos\theta ds} = \frac{1}{2M_\Lambda^3}\frac{2\beta\sqrt{\lambda}}{(8\pi)^3}|\mathcal{M}^{\rm tot}|^2, \quad (17)$$

where $\beta \equiv \sqrt{1-\frac{4m_\ell^2}{s}}$ and $\lambda = \lambda(M_{\Lambda_b}, M_\Lambda, s) \equiv M_{\Lambda_b}^4 + M_\Lambda^4 + s^2 - 2M_{\Lambda_b}^2 M_\Lambda^2 - 2sM_{\Lambda_b}^2 - 2sM_\Lambda^2$. Also, s is the square of the momentum transfer q and θ is the angle between the lepton and final-state baryon in the rest frame of Λ_b. By using the expression of amplitude given in Eq. (13) and integration over $\cos\theta$, one can get the expression of the dilepton invariant mass spectrum as

$$\frac{d\Gamma(\Lambda_b \to \Lambda\ell^+\ell^-)}{ds} = \frac{G_{\rm F}^2\alpha_{\rm EM}^2\beta\sqrt{\lambda}}{2^{13}\pi^5 M_{\Lambda_b}^3}|V_{tb}V_{ts}^*|^2\mathcal{M}_1, \quad (18)$$

with

$$\begin{aligned}\mathcal{M}_1 = \Bigg\{ & \frac{8}{3}\left(\left(3\Delta_1 + \left(\frac{4m_\ell^2\lambda}{s} - \lambda\right)\right)\left(|A|^2 + |D|^2\right) + 12m_\ell^2\left(\Delta|A|^2 + \omega|D|^2\right)\right. \\ & + 3s\left(\Delta_1|B|^2 + \Delta_2|E|^2\right) + \left(12m_\ell^2\Delta_3 + \lambda\left(s - 4m_\ell^2\right)\right)\left(|B|^2 + |E|^2\right) + 3\left(\Delta_1|G|^2 + \Delta_2|J|^2\right) \\ & - 12m_\ell^2\left(\Delta|G|^2 - \omega|J|^2\right) - 48m_\ell^2 M_{\Lambda_b} M_\Lambda\left(|G|^2 - |J|^2\right) - \left(\lambda - \frac{4m_\ell^2\lambda}{s}\right)\left(|G|^2 + |J|^2\right) \\ & \left. + \left(s - 4m_\ell^2\right)\left(|H|^2\left(3\Delta_1 + \lambda\right) + |K|^2(3\Delta_2 + \lambda)\right)\right) + 32m_\ell^2 s\left(\omega|I|^2 + \Delta|L|^2\right) \\ & - 16\Delta\left(M_{\Lambda_b} + M_\Lambda\right)\left(s + 2m_\ell^2\right)\left(AB^* + BA^*\right) - 16\omega\left(s - 4m_\ell^2\right)\left(M_{\Lambda_b} - M_\Lambda\right)\left(JK^* + KJ^*\right) \\ & - 32m_\ell^2\Delta\left(M_{\Lambda_b} + M_\Lambda\right)\left(JL^* + LJ^*\right) + 16\omega\left(s + 2m_\ell^2\right)\left(M_{\Lambda_b} - M_\Lambda\right)\left(DE^* + ED^*\right)\Bigg\},\end{aligned} \tag{19}$$

where

$$\begin{aligned}\Delta &\equiv \left(M_\Lambda - M_{\Lambda_b}\right)^2 - s \\ \omega &\equiv \left(M_\Lambda + M_{\Lambda_b}\right)^2 - s \\ \omega_1 &\equiv \left(M_\Lambda + M_{\Lambda_b}\right)^2 + s \\ \omega_2 &\equiv \left(M_\Lambda - M_{\Lambda_b}\right)^2 + s \\ \omega_3 &\equiv \left(M_{\Lambda_b}^2 - M_\Lambda^2 + 6M_{\Lambda_b}M_\Lambda - s\right) \\ \omega_4 &\equiv \left(M_{\Lambda_b}^2 - M_\Lambda^2 - 6M_{\Lambda_b}M_\Lambda - s\right) \\ \Delta_1 &\equiv \left(M_\Lambda^2 - M_{\Lambda_b}^2\right)^2 - s\left(4M_{\Lambda_b}M_\Lambda + s\right) \\ \Delta_2 &\equiv \left(M_\Lambda^2 - M_{\Lambda_b}^2\right)^2 + s\left(4M_{\Lambda_b}M_\Lambda - s\right) \\ \Delta_3 &\equiv \left(M_{\Lambda_b}^2 - M_\Lambda^2\right)^2 - s\left(M_{\Lambda_b} - M_\Lambda\right)^2 \\ \Delta_4 &\equiv \left(M_{\Lambda_b}^2 - M_\Lambda^2\right)^2 + s\left(M_{\Lambda_b} - M_\Lambda\right)^2.\end{aligned}$$

Following the recipe given in Ref. [12], one can define the CP-violation asymmetry for the polarized and unpolarized leptons in $\Lambda_b \to \Lambda\ell^+\ell^-$ decay as

$$\mathcal{A}_{\rm CP}\left(\mathbf{S}^\pm = \mathbf{e}_i^\pm\right) = \frac{\frac{d\Gamma\left(\mathbf{S}^-\right)}{ds} - \frac{d\bar{\Gamma}\left(\mathbf{S}^+\right)}{ds}}{\frac{d\Gamma\left(\mathbf{S}^-\right)}{ds} + \frac{d\bar{\Gamma}\left(\mathbf{S}^+\right)}{ds}}, \tag{20}$$

where

$$\begin{aligned}\frac{d\Gamma\left(S^-\right)}{ds} &= \frac{d\Gamma\left(\Lambda_b \to \Lambda\ell^+\ell^-\left(S^-\right)\right)}{ds} \\ \frac{d\bar{\Gamma}\left(S^+\right)}{ds} &= \frac{d\bar{\Gamma}\left(\Lambda_b \to \Lambda\ell^+\ell^-\left(S^+\right)\right)}{ds}.\end{aligned}$$

An analogous expression for the CP-conjugated differential decay width is given in Ref. [12]. The expression for CP-violation asymmetry can be obtained by using Eqs. (18) and (19) as

$$\mathcal{A}_{\rm CP}\big(\mathbf{S}^{\pm}=\mathbf{e}_i^{\pm}\big)=\tfrac{1}{2}\left[\frac{\mathcal{M}_1-\bar{\mathcal{M}}_1}{\mathcal{M}_1+\bar{\mathcal{M}}_1}\pm\frac{\mathcal{M}_1^i-\bar{\mathcal{M}}_1^i}{\mathcal{M}_1^i+\bar{\mathcal{M}}_1^i}\right], \tag{21}$$

where i represents the longitudinal (L), normal (N), and transverse (T) polarization of the final-state leptons.

Also, one can write the polarized and unpolarized CP asymmetries as

$$\mathcal{A}_{\rm CP}(s)=\frac{\mathcal{M}_1-\bar{\mathcal{M}}_1}{\mathcal{M}_1+\bar{\mathcal{M}}_1},\quad \mathcal{A}^i_{\rm CP}(s)=\frac{\mathcal{M}_1^i-\bar{\mathcal{M}}_1^i}{\mathcal{M}_1^i+\bar{\mathcal{M}}_1^i}. \tag{22}$$

The normalized CP-violation asymmetry can be defined by using the above definition as follows:

$$\mathcal{A}_{\rm CP}\big(\mathbf{S}^{\pm}=e_i^{\pm}\big)=\tfrac{1}{2}\Big[\mathcal{A}_{\rm CP}(s)\pm\mathcal{A}^i_{\rm CP}(s)\Big]. \tag{23}$$

In Eq. (23) the positive sign represents the longitudinal (L) and normal (N) polarizations, and the negative sign is for the transverse (T) polarization.

Finally, the results for unpolarized $\mathcal{A}_{\rm CP}$ and polarized $\mathcal{A}^i_{\rm CP}$ are [12]

$$\mathcal{A}_{\rm CP}(s)=\frac{-2\mathcal{I}m(\Lambda_{sb})\mathcal{Q}(s)}{\mathcal{M}_1+2\mathcal{I}m\big(\Lambda_{sb}\big)\mathcal{Q}(s)}, \tag{24}$$

$$\mathcal{A}^i_{\rm CP}(s)=\frac{-2\mathcal{I}m(\Lambda_{sb})\mathcal{Q}^i(s)}{\mathcal{M}_1+2\mathcal{I}m\big(\Lambda_{sb}\big)\mathcal{Q}^i(s)}. \tag{25}$$

Here

$$\mathcal{Q}(s)=\frac{16}{3s}\left\{\mathcal{H}_1\mathcal{I}m\Big(C_7C_9^{Z^{*\prime}}\Big)-\mathcal{H}_2\mathcal{I}m\Big(C_9C_9^{Z^{*\prime}}\Big)+\mathcal{H}_3\mathcal{I}m\Big(C_{10}C_{10}^{Z^{*\prime}}\Big)\right\} \tag{26}$$

and the explicit form of the functions $\mathcal{H}_1$, $\mathcal{H}_2$, and $\mathcal{H}_3$ can be written as

$$\begin{aligned}\mathcal{H}_1=&\Big\{\lambda s\big(s-4m_\ell^2\big)\big(\mathcal{D}_4\mathcal{D}_3^*-\mathcal{D}_{10}\mathcal{D}_9^*\big)-6s\Delta\big(M_{\Lambda_b}+M_\Lambda\big)\big(s+2m_\ell^2\big)\big(\mathcal{D}_4\mathcal{D}_1^*+\mathcal{D}_2\mathcal{D}_3^*\big)\\&+6s\omega\big(M_{\Lambda_b}-M_\Lambda\big)\big(s+2m_\ell^2\big)\big(\mathcal{D}_{10}\mathcal{D}_7^*-\mathcal{D}_8\mathcal{D}_9^*\big)\\&+3s\big(s+4m_\ell^2\big)\big((\Delta_1+\Delta_3)\mathcal{D}_4\mathcal{D}_3^*-\big(\Delta_2+\Delta_4\big)\mathcal{D}_{10}\mathcal{D}_9^*\big)\\&+3s\big(\Delta\big(\omega_1+4m_\ell^2\big)\mathcal{D}_2\mathcal{D}_1^*+\omega\big(\omega_2+4m_\ell^2\big)\mathcal{D}_8\mathcal{D}_7^*\big)-\lambda\big(s-4m_\ell^2\big)\big(\mathcal{D}_2\mathcal{D}_1^*+\mathcal{D}_8\mathcal{D}_7^*\big)\Big\}\end{aligned} \tag{27}$$

$$\begin{aligned}\mathcal{H}_2=&\Big\{3s\big(\Delta\big(\omega_1+4m_\ell^2\big)|\mathcal{D}_1|^2+\omega\big(\omega_2+4m_\ell^2\big)|\mathcal{D}_7|^2\big)+\lambda s\big(s-4m_\ell^2\big)\big(|\mathcal{D}_3|^2+|\mathcal{D}_9|^2\big)\\&-6s\Delta\big(M_{\Lambda_b}+M_\Lambda\big)\big(s+2m_\ell^2\big)\big(\mathcal{D}_1\mathcal{D}_3^*+\mathcal{D}_3\mathcal{D}_1^*\big)+3s\big(s+4m_\ell^2\big)\big(\Delta_1|\mathcal{D}_3|^2+\Delta_4|\mathcal{D}_9|^2\big)\\&-6s\omega\big(M_{\Lambda_b}-M_\Lambda\big)\big(s+2m_\ell^2\big)\big(\mathcal{D}_7\mathcal{D}_9^*+\mathcal{D}_9\mathcal{D}_7^*\big)\Big\}\end{aligned} \tag{28}$$

$$\begin{aligned}\mathcal{H}_3=&\Big\{\lambda s\big(s-4m_\ell^2\big)\big(|\mathcal{D}_1|^2+|\mathcal{D}_7|^2\big)+3s(\lambda_1|\mathcal{D}_1|^2+\lambda_2|\mathcal{D}_7|^2)\\&+6s\Delta\big(M_{\Lambda_b}+M_\Lambda\big)\big(s-4m_\ell^2\big)\big(\mathcal{D}_1\mathcal{D}_3^*+\mathcal{D}_3\mathcal{D}_1^*\big)\\&+12sm_\ell^2\Delta\big(M_{\Lambda_b}+M_\Lambda\big)\big(\mathcal{D}_7\mathcal{D}_{11}^*+\mathcal{D}_{11}\mathcal{D}_7^*\big)-3s\big(s-4m_\ell^2\big)\big(\Delta_1|\mathcal{D}_3|^2+\Delta_2|\mathcal{D}_9|^2\big)\\&-12s^2m_\ell^2\big(\omega|\mathcal{D}_5|^2+\Delta|\mathcal{D}_{11}|^2\big)-\lambda s\big(s-4m_\ell^2\big)\big(|\mathcal{D}_3|^2+|\mathcal{D}_9|^2\big)\\&-6s\omega\big(M_{\Lambda_b}-M_\Lambda\big)\big(s-4m_\ell^2\big)\big(\mathcal{D}_9\mathcal{D}_7^*+\mathcal{D}_7\mathcal{D}_9^*\big)+2s\omega m_\ell^2\big(M_{\Lambda_b}-M_\Lambda\big)\mathcal{D}_1\mathcal{D}_5^*\Big\}.\end{aligned} \tag{29}$$

The expressions for polarized CP-violation asymmetry for different possible lepton polarizations are given below.

2.1. Longitudinal CP-violation asymmetry

The CP-violation asymmetry corresponding to longitudinal lepton polarization can be written as

$$\mathcal{A}_{\rm CP}^{L}(s) = \frac{-2\mathcal{I}m\big(\Lambda_{sb}\big)\mathcal{Q}^{L}(s)}{\mathcal{M}_1 + 2\mathcal{I}m\big(\Lambda_{sb}\big)\mathcal{Q}^{L}(s)}, \tag{30}$$

with

$$\mathcal{Q}^{L} = \frac{8}{3}\left\{\frac{1}{s}\Big(\mathcal{H}_1^{L}\mathcal{I}m\Big(C_7C_9^{Z^{*\prime}}\Big) - \mathcal{H}_2^{L}\mathcal{I}m\Big(C_9C_9^{Z^{*\prime}}\Big) + \mathcal{H}_3^{L}\mathcal{I}m\Big(C_{10}C_{10}^{Z^{*\prime}}\Big)\Big) + \frac{1}{\sqrt{s}}\Big(\mathcal{H}_4^{L}\mathcal{I}m\Big(C_7C_{10}^{Z^{*\prime}}\Big) - \mathcal{H}_5^{L}\mathcal{I}m\Big(C_9C_{10}^{Z^{*\prime}}\Big)\Big)\right\}, \tag{31}$$

where $\mathcal{H}_1^{L} = \mathcal{H}_1$, $\mathcal{H}_2^{L} = \mathcal{H}_2$, and $\mathcal{H}_3^{L} = \mathcal{H}_3$. Also, $\mathcal{M}_1$ is defined in Eq. (19) and the terms $\mathcal{H}_4^{L}$ and $\mathcal{H}_5^{L}$ are given as follows:

$$\mathcal{H}_4^{L} = \sqrt{s-4m_\ell^2}\Big\{3s\big(\Delta_1(\mathcal{D}_4\mathcal{D}_3^*) - \Delta_2\big(\mathcal{D}_{10}\mathcal{D}_9^*\big)\big) + \lambda s\big(\mathcal{D}_4\mathcal{D}_3^* - \mathcal{D}_{10}\mathcal{D}_9^*\big) - 6s\Delta\big(M_{\Lambda_b} + M_\Lambda\big)\big(\mathcal{D}_2\mathcal{D}_3^* + \mathcal{D}_4\mathcal{D}_1^*\big) - 6s\omega\big(M_{\Lambda_b} - M_\Lambda\big)\big(\mathcal{D}_8\mathcal{D}_9^* + \mathcal{D}_{10}\mathcal{D}_7^*\big) + \big(3\Delta_2 - \lambda\big)\big(\mathcal{D}_2\mathcal{D}_1^* + \mathcal{D}_8\mathcal{D}_7^*\big)\Big\} \tag{32}$$

$$\mathcal{H}_5^{L} = \sqrt{s-4m_\ell^2}\Big\{\big(\big(3\Delta_1 - \lambda\big)|\mathcal{D}_1|^2 - \big(3\Delta_2 + \lambda\big)|\mathcal{D}_7|^2 - 6s\Delta\big(M_{\Lambda_b} + M_\Lambda\big)\big(\mathcal{D}_1\mathcal{D}_3^* + \mathcal{D}_3\mathcal{D}_1^*\big) + 6s\omega\big(M_{\Lambda_b} - M_\Lambda\big)\big(\mathcal{D}_7\mathcal{D}_9^* + \mathcal{D}_9\mathcal{D}_7^*\big) + s\big(\big(3\Delta_1 + \lambda\big)|\mathcal{D}_3|^2 + \big(3\Delta_2 + \lambda\big)|\mathcal{D}_9|^2\big)\Big\}. \tag{33}$$

2.2. Normal CP-violation asymmetry

In the case of the normally polarized lepton, the corresponding normal CP violation can be expressed as

$$\mathcal{A}_{\rm CP}^{N}(s) = \frac{-2\mathcal{I}m\big(\Lambda_{sb}\big)\mathcal{Q}^{N}(s)}{\mathcal{M}_1 + 2\mathcal{I}m\big(\Lambda_{sb}\big)\mathcal{Q}^{N}(s)}, \tag{34}$$

where

$$\mathcal{Q}^{N} = \left\{\frac{8}{3s}\Big(\mathcal{H}_1^{N}\mathcal{I}m\Big(C_7C_9^{Z^{*\prime}}\Big) - \mathcal{H}_2^{N}\mathcal{I}m\Big(C_9C_9^{Z^{*\prime}}\Big) + \mathcal{H}_3^{N}\mathcal{I}m\Big(C_{10}C_{10}^{Z^{*\prime}}\Big)\Big) + \frac{4\pi\sqrt{\lambda}}{\sqrt{s}}\Big(\mathcal{H}_4^{N}\mathcal{I}m(C_9C_{10}^{Z^{*\prime}}\Big) + \mathcal{H}_5^{N}\mathcal{I}m\Big(C_{10}C_9^{Z^{*\prime}}\Big) - \mathcal{H}_6^{N}\mathcal{I}m\Big(C_7C_{10}^{Z^{*\prime}}\Big)\Big)\right\} \tag{35}$$

and

$$\begin{aligned}\mathcal{H}_1^{N} = {} & 3\pi\sqrt{\lambda}m_\ell s^{3/2}\big(\big(M_{\Lambda_b} - M_\Lambda\big)\big(\mathcal{D}_{10}\mathcal{D}_1^* - \mathcal{D}_2\mathcal{D}_9^*\big) - \big(\mathcal{D}_8\mathcal{D}_1^* - \mathcal{D}_2\mathcal{D}_7^*\big)\big) \\ & + 3\pi\sqrt{\lambda}m_\ell s^{3/2}\big(\big(M_{\Lambda_b}^2 - M_\Lambda^2\big)\big(\mathcal{D}_4\mathcal{D}_9^* - \mathcal{D}_{10}\mathcal{D}_3^*\big) + \big(M_{\Lambda_b} + M_\Lambda\big)\big(\mathcal{D}_4\mathcal{D}_7^* + \mathcal{D}_8\mathcal{D}_3^*\big)\big) \\ & + 6s\Delta\big(s + 2m_\ell^2\big)\big(M_{\Lambda_b} + M_\Lambda\big)\big(\mathcal{D}_2\mathcal{D}_3^* - \mathcal{D}_4\mathcal{D}_1^*\big) + \lambda s\big(s - 4m_\ell^2\big)\big(\mathcal{D}_4\mathcal{D}_3^* - \mathcal{D}_{10}\mathcal{D}_9^* - \mathcal{D}_2\mathcal{D}_1^*\big) \\ & + 3s\big(s + 4m_\ell^2\big)\big(\big(\Delta_1 + \Delta_3\big)\mathcal{D}_4\mathcal{D}_3^* - \big(\Delta_2 + \Delta_4\big)\mathcal{D}_{10}\mathcal{D}_9^*\big) - \lambda\big(s - 4m_\ell^2\big)\mathcal{D}_8\mathcal{D}_7^* \\ & + 6\omega s\big(s + 2m_\ell^2\big)\big(M_{\Lambda_b} - M_\Lambda\big)\big(\mathcal{D}_8\mathcal{D}_9^* - \mathcal{D}_{10}\mathcal{D}_7^*\big) \\ & + 3s\big(\Delta\big(\omega_1 + 4m_\ell^2\big)\mathcal{D}_2\mathcal{D}_1^* + \omega\big(\omega_2 + 4m_\ell^2\big)\mathcal{D}_8\mathcal{D}_7^*\big)\end{aligned} \tag{36}$$

$$\begin{aligned}\mathcal{H}_2^N &= \Big\{3\pi\sqrt{\lambda}m_\ell s^{3/2}\big((M_{\Lambda_b}+M_\Lambda)(\mathcal{D}_7\mathcal{D}_3^*+\mathcal{D}_3\mathcal{D}_7^*)-(M_{\Lambda_b}-M_\Lambda)(\mathcal{D}_1\mathcal{D}_9^*-\mathcal{D}_9\mathcal{D}_1^*)\big)\\ &\quad -3\pi\sqrt{\lambda}m_\ell s^{3/2}(\mathcal{D}_1\mathcal{D}_7^*+\mathcal{D}_7\mathcal{D}_1^*)-6s\Delta(s+2m_\ell^2)(M_{\Lambda_b}+M_\Lambda)(\mathcal{D}_1\mathcal{D}_3^*+\mathcal{D}_3\mathcal{D}_1^*)\\ &\quad -\lambda(s-4m_\ell^2)(|\mathcal{D}_1|^2+|\mathcal{D}_7|^2)+6\omega s(s+2m_\ell^2)(M_{\Lambda_b}-M_\Lambda)(\mathcal{D}_7\mathcal{D}_9^*+\mathcal{D}_9\mathcal{D}_7^*)\\ &\quad +3s\big(\Delta(\omega_1+4m_\ell^2)|\mathcal{D}_1|^2+\omega(\omega_2+4m_\ell^2)|\mathcal{D}_7|^2\big)+3s(s+4m_\ell^2)\big((\Delta_1+\Delta_3)|\mathcal{D}_3|^2\\ &\quad +(\Delta_2+\Delta_4)|\mathcal{D}_9|^2+\lambda s(s-4m_\ell^2)(|\mathcal{D}_3|^2+|\mathcal{D}_9|^2)+3\pi\sqrt{\lambda}m_\ell s^{3/2}(M_{\Lambda_b}^2-M_\Lambda^2)\mathcal{D}_3\mathcal{D}_9^*\Big\}\end{aligned} \tag{37}$$

$$\begin{aligned}\mathcal{H}_4^N &= m_\ell\Big\{s^2(\mathcal{D}_3\mathcal{D}_5^*+\mathcal{D}_9\mathcal{D}_{11}^*)-(M_{\Lambda_b}^2-M_\Lambda^2)(|\mathcal{D}_1|^2+|\mathcal{D}_7|^2)-s(\mathcal{D}_1\mathcal{D}_5^*+\mathcal{D}_7\mathcal{D}_{11}^*)\\ &\quad +s\big((M_{\Lambda_b}-M_\Lambda)\mathcal{D}_3\mathcal{D}_1^*-(M_{\Lambda_b}+M_\Lambda)\mathcal{D}_9\mathcal{D}_7^*\big)\Big\}\end{aligned} \tag{38}$$

$$\begin{aligned}\mathcal{H}_5^N &= m_\ell\Big\{s(M_{\Lambda_b}+M_\Lambda)(\mathcal{D}_5\mathcal{D}_1^*+\mathcal{D}_7\mathcal{D}_9^*)+s(M_{\Lambda_b}-M_\Lambda)(\mathcal{D}_{11}\mathcal{D}_7^*+\mathcal{D}_5\mathcal{D}_1^*)\\ &\quad -(M_{\Lambda_b}^2-M_\Lambda^2)(|\mathcal{D}_1|^2+|\mathcal{D}_7|^2)+s^2(\mathcal{D}_{11}\mathcal{D}_9^*+\mathcal{D}_5\mathcal{D}_3^*)\Big\}\end{aligned} \tag{39}$$

$$\begin{aligned}\mathcal{H}_6^N &= m_\ell\Big\{s(M_{\Lambda_b}-M_\Lambda)(\mathcal{D}_8\mathcal{D}_{11}^*-\mathcal{D}_4\mathcal{D}_1^*)+s^2(\mathcal{D}_4\mathcal{D}_5^*-\mathcal{D}_{10}\mathcal{D}_{11}^*)\\ &\quad +s(M_{\Lambda_b}+M_\Lambda)(\mathcal{D}_{10}\mathcal{D}_7^*-\mathcal{D}_2\mathcal{D}_5^*)-(M_{\Lambda_b}^2-M_\Lambda^2)(\mathcal{D}_2\mathcal{D}_1^*+\mathcal{D}_8\mathcal{D}_7^*)\Big\}.\end{aligned} \tag{40}$$

2.3. Transverse CP-violation asymmetry

The transverse CP-violation asymmetry can be written as

$$\mathcal{A}_{\rm CP}^T(s)=\frac{-2\mathcal{I}m(\Lambda_{sb})\mathcal{Q}^T(s)}{\mathcal{M}_1+2\mathcal{I}m(\Lambda_{sb})\mathcal{Q}^T(s)} \tag{41}$$

with

$$\begin{aligned}\mathcal{Q}^T(s) &= \Bigg\{\frac{8}{3s}\Big(\mathcal{H}_1^T\mathcal{I}m\Big(C_7C_9^{Z^{*\prime}}\Big)-\mathcal{H}_2^T\mathcal{I}m\Big(C_9C_9^{Z^{*\prime}}\Big)\Big)+4\pi\sqrt{\lambda\Big(s-4m_\ell^2\Big)}\Big(\mathcal{H}_3^T\mathcal{R}e\Big(C_9C_{10}^{Z^{*\prime}}\Big)\\ &\quad +\mathcal{H}_4^T\mathcal{R}e\Big(C_{10}C_9^{Z^{*\prime}}\Big)-\mathcal{H}_5^T\mathcal{R}e\Big(C_7C_{10}^{Z^{*\prime}}\Big)\Big)\\ &\quad +\frac{4}{3s}\Big(\mathcal{H}_6^{T^A}\mathcal{I}m\Big(C_{10}C_{10}^{Z^{*\prime}}\Big)+\mathcal{H}_6^{T^B}\mathcal{R}e\Big(C_{10}C_{10}^{Z^{*\prime}}\Big)\Big)\Bigg\},\end{aligned} \tag{42}$$

where $\mathcal{H}_1^T=\mathcal{H}_1^L$, $\mathcal{H}_2^T=\mathcal{H}_3^L$, $\mathcal{H}_6^{T^A}=\Big(\mathcal{H}_6^{T^1}+\mathcal{H}_6^{T^2}+\mathcal{H}_6^{T^3}\Big)$, and $\mathcal{H}_6^{T^B}=\Big(\mathcal{H}_6^{T^4}+\mathcal{H}_6^{T^5}\Big)$.

The different terms given in the above equation can be expressed as:

$$\begin{aligned}\mathcal{H}_3^T &= m_\ell\Big\{(M_{\Lambda_b}+M_\Lambda)(\mathcal{D}_3\mathcal{D}_7^*+\mathcal{D}_7\mathcal{D}_3^*)+(M_{\Lambda_b}^2-M_\Lambda^2)(\mathcal{D}_3\mathcal{D}_9^*+\mathcal{D}_9\mathcal{D}_3^*)\\ &\quad +s(\mathcal{D}_3\mathcal{D}_9^*-\mathcal{D}_9\mathcal{D}_3^*)\Big\}\end{aligned} \tag{43}$$

$$\begin{aligned}\mathcal{H}_4^T &= m_\ell\Big\{(M_{\Lambda_b}-M_\Lambda)(\mathcal{D}_1\mathcal{D}_9^*+\mathcal{D}_9\mathcal{D}_1^*)-(M_{\Lambda_b}^2-M_\Lambda^2)(\mathcal{D}_3\mathcal{D}_9^*-\mathcal{D}_9\mathcal{D}_3^*)\\ &\quad +s(\mathcal{D}_3\mathcal{D}_9^*-\mathcal{D}_9\mathcal{D}_3^*)-(M_{\Lambda_b}+M_\Lambda)(\mathcal{D}_3\mathcal{D}_7^*+\mathcal{D}_7\mathcal{D}_3^*)\Big\}\end{aligned} \tag{44}$$

$$\mathcal{H}_5^T = m_\ell\Big\{\big(M_{\Lambda_b}+M_\Lambda\big)\big(\mathcal{D}_4\mathcal{D}_7^*+\mathcal{D}_8\mathcal{D}_3^*\big)+\big(M_{\Lambda_b}^2-M_\Lambda^2+s\big)\big(\mathcal{D}_4\mathcal{D}_9^*-\mathcal{D}_{10}\mathcal{D}_3^*\big) + \big(M_{\Lambda_b}-M_\Lambda\big)\big(\mathcal{D}_{10}\mathcal{D}_1^*-\mathcal{D}_2\mathcal{D}_1^*\big)\Big\} \tag{45}$$

$$\begin{aligned}\mathcal{H}_6^{T^1} = {}& \Big\{\big(6s^4-24s^3m_\ell^2-24s^3M_{\Lambda_b}M_\Lambda+2s^2\Delta_5\big)\big(|\mathcal{D}_3|^2+|\mathcal{D}_9|^2\big)+24s^3m_\ell^2\big(|\mathcal{D}_5|^2+|\mathcal{D}_{11}|^2\big)\\ &+12s^3\big(\big(M_{\Lambda_b}-M_\Lambda\big)\mathcal{D}_9\mathcal{D}_7^*-\big(M_{\Lambda_b}+M_\Lambda\big)\mathcal{D}_3\mathcal{D}_1^*\big)+48m_\ell^2M_{\Lambda_b}M_\Lambda\big(|\mathcal{D}_3|^2-|\mathcal{D}_9|^2\big)\\ &+12m_\ell^2\big(\big(M_{\Lambda_b}+M_\Lambda\big)\big(2\mathcal{D}_3\mathcal{D}_1^*+\mathcal{D}_{11}\mathcal{D}_7^*\big)+\big(M_{\Lambda_b}-M_\Lambda\big)\big(2\mathcal{D}_9\mathcal{D}_7^*-\mathcal{D}_5\mathcal{D}_1^*\big)\big)\\ &+12m_\ell^2\big(M_{\Lambda_b}\big(M_{\Lambda_b}+M_\Lambda\big)|\mathcal{D}_5|^2-\big(M_{\Lambda_b}-M_\Lambda\big)^2|\mathcal{D}_{11}|^2\big)\\ &+6\big(M_{\Lambda_b}^2-M_\Lambda^2\big)\big(\big(M_{\Lambda_b}+M_\Lambda\big)\mathcal{D}_9\mathcal{D}_7^*-\big(M_{\Lambda_b}-M_\Lambda\big)\mathcal{D}_3\mathcal{D}_1^*\big)\Big\}\end{aligned} \tag{46}$$

$$\begin{aligned}\mathcal{H}_6^{T^2} = {}& 8m_\ell^2s\Big\{3\big(M_{\Lambda_b}^2-M_\Lambda^2\big)\big(\big(M_{\Lambda_b}^2-M_\Lambda^2\big)\big(|\mathcal{D}_3|^2+|\mathcal{D}_9|^2\big)+\big(M_{\Lambda_b}+M_\Lambda\big)\big(\mathcal{D}_5\mathcal{D}_1^*-2\mathcal{D}_9\mathcal{D}_7^*\big)\\ &+\big(M_{\Lambda_b}-M_\Lambda\big)\big(2\mathcal{D}_3\mathcal{D}_1^*-\mathcal{D}_{11}\mathcal{D}_7^*\big)\big)+\lambda\big(|\mathcal{D}_3|^2+|\mathcal{D}_9|^2\big)\Big\}\end{aligned} \tag{47}$$

$$\begin{aligned}\mathcal{H}_6^{T^3} = {}& \Big\{\big(2s\lambda-8m_\ell^2\lambda\big)\big(|\mathcal{D}_1|^2+|\mathcal{D}_7|^2\big)+\big(24sm_\ell^2-6s\big)\big(\Delta_1|\mathcal{D}_1|^2-\Delta_2|\mathcal{D}_7|^2\big)\\ &+24sm_\ell^2\big(\omega_4|\mathcal{D}_1|^2+\omega_3|\mathcal{D}_7|^2\big)+12s\big(s-4m_\ell^2\big)\big(\Delta\big(M_{\Lambda_b}+M_\Lambda\big)\mathcal{D}_1\mathcal{D}_3^*\\ &-\omega\big(M_{\Lambda_b}-M_\Lambda\big)\mathcal{D}_7\mathcal{D}_9^*\big)+24sm_\ell^2\big(\Delta\big(M_{\Lambda_b}+M_\Lambda\big)\mathcal{D}_7\mathcal{D}_{11}^*+\omega\big(M_{\Lambda_b}-M_\Lambda\big)\mathcal{D}_1\mathcal{D}_5^*\big)\Big\}\end{aligned} \tag{48}$$

$$\mathcal{H}_6^{T^4} = 3m_\ell\pi s^2\sqrt{\lambda(s-4m_\ell^2)}\big\{\big(|\mathcal{D}_3|^2+|\mathcal{D}_9|^2\big)-\big(\mathcal{D}_3\mathcal{D}_5^*+\mathcal{D}_5\mathcal{D}_3^*\big)+\big(\mathcal{D}_9\mathcal{D}_{11}^*-\mathcal{D}_{11}\mathcal{D}_9^*\big)\big\} \tag{49}$$

$$\begin{aligned}\mathcal{H}_6^{T^5} = {}& 3m_\ell\pi s\sqrt{\lambda\big(s-4m_\ell^2\big)}\Big\{\big(M_{\Lambda_b}+M_\Lambda\big)\big(\mathcal{D}_3\mathcal{D}_1^*+\mathcal{D}_1\mathcal{D}_5^*-\mathcal{D}_9\mathcal{D}_7^*\big)\\ &+\big(M_{\Lambda_b}-M_\Lambda\big)\big(\mathcal{D}_7\mathcal{D}_{11}^*-\mathcal{D}_{11}\mathcal{D}_7^*\big)-\big(M_{\Lambda_b}^2-M_\Lambda^2\big)\big(|\mathcal{D}_3|^2+|\mathcal{D}_9|^2\big)-\big(|\mathcal{D}_1|^2+|\mathcal{D}_7|^2\big)\Big\},\end{aligned} \tag{50}$$

where $\mathcal{D}_{1,3,5}=f_{1,2,3}$, $\mathcal{D}_{2,4,6}=\frac{2m_b}{s}f_{1,2,3}^T$ and $\mathcal{D}_{7,9,11}=g_{1,2,3}$, $\mathcal{D}_{8,10,12}=\frac{2m_b}{s}g_{1,2,3}^T$.

3. Numerical analysis

In this section we will discuss numerically the unpolarized and polarized CP-violation asymmetries for $\Lambda_b\to\Lambda\ell^+\ell^-$, with $\ell=\mu,\tau$, decays. In order to see the imprints of the family non-universal Z' gauge boson on the above-mentioned physical observables, first we summarize the numerical values of various input parameters used in the calculations, such as masses of particles, lifetime, quark-coupling CKM matrix etc., in Table 1, while the values of the Wilson coefficients are presented in Table 2. The most important input parameters in hadronic decays are the form factors that are non-perturbative quantities. In order to calculate these non-perturbative quantities, one has to rely on some model and, in the present case, we will use the form factors calculated using the light-cone QCD sum rules approach [90]. The parameterization of the form factors $f_{1,2,3}$, $g_{1,2,3}$, $f_{2,3}^T$, and $g_{2,3}^T$ is given by

$$f_i\big(q^2\big)\big[g_i\big(q^2\big)\big]=\frac{a}{1-q^2/m_{\rm fit}^2}+\frac{b}{\big(1-q^2/m_{\rm fit}^2\big)^2}, \tag{51}$$

Table 1. Default values of input parameters used in the calculations.

Parameter	Value
M_{Λ_b}	5.620 GeV
m_b	4.28 GeV
m_s	0.13 GeV
m_μ	0.105 GeV
m_τ	1.77 GeV
$\lvert V_{tb}V_{ts}^*\rvert$	45×10^{-3}
α^{-1}	137
$G_{\rm F}$	$1.17 \times 10^{-5}\,{\rm GeV}^{-2}$
τ_{Λ_b}	1.383×10^{-12} s
M_Λ	1.115 GeV

Table 2. The Wilson coefficients C_i^μ at the scale $\mu \sim m_b$ in the SM [6].

C_1	C_2	C_3	C_4	C_5	C_6	C_7	C_9	C_{10}
1.107	−0.248	−0.011	−0.026	−0.007	−0.031	−0.313	4.344	−4.669

Table 3. Fit parameters for the $\Lambda_b \to \Lambda \ell^- \ell^-$ transition form factors in full theory. Here only the central value is given [90].

	a	b	$m_{\rm fit}^2$
f_1	−0.046	0.368	39.10
f_2	0.0046	−0.017	26.37
f_3	0.006	−0.021	22.99
g_1	−0.220	0.538	48.70
g_2	0.005	−0.018	26.93
g_3	0.035	−0.050	24.26
f_2^T	−0.131	0.426	45.70
f_3^T	−0.046	0.102	28.31
g_2^T	−0.369	0.664	59.37
f_2^T	−0.026	−0.075	23.73

Table 4. Fit parameters for the $\Lambda_b \to \Lambda \ell^- \ell^-$ transition form factors in full theory for f_1^T and g_1^T. Here only the central value is given [90].

	c	$m_{\rm fit}^{\prime 2}$	$m_{\rm fit}^{\prime\prime 2}$
f_1^T	−1.191	23.81	59.96
g_1^T	−0.653	24.15	48.52

while the form factors f_1^T and g_1^T are of the form

$$f_1^T\left[g_1^T\right] = \frac{c}{1 - q^2/m_{\rm fit}^{\prime 2}} + \frac{c}{\left(1 - q^2/m_{\rm fit}^{\prime\prime 2}\right)^2}. \tag{52}$$

The numerical values of the light-cone QCD sum rule form factors along with the different fitting parameters [90] are summarized in Tables 3 and 4.

Now the next step is to collect the values of the Z' couplings and, in this regard, there are some severe constraints from different inclusive and exclusive B decays [32]. These numerical values for

Table 5. The numerical values of the Z' parameters [32,38–44,91,101].

	$\lvert\mathcal{B}_{sb}\rvert \times 10^{-3}$	ϕ_{sb} (in degrees)	$S_{LL} \times 10^{-2}$	$D_{LL} \times 10^{-2}$
$\mathcal{S}1$	1.09 ± 0.22	-72 ± 7	-2.8 ± 3.9	-6.7 ± 2.6
$\mathcal{S}2$	2.20 ± 0.15	-82 ± 4	-1.2 ± 1.4	-2.5 ± 0.9
$\mathcal{S}3$	4.0 ± 1.5	150 ± 10 or (-150 ± 10)	0.8	-2.6

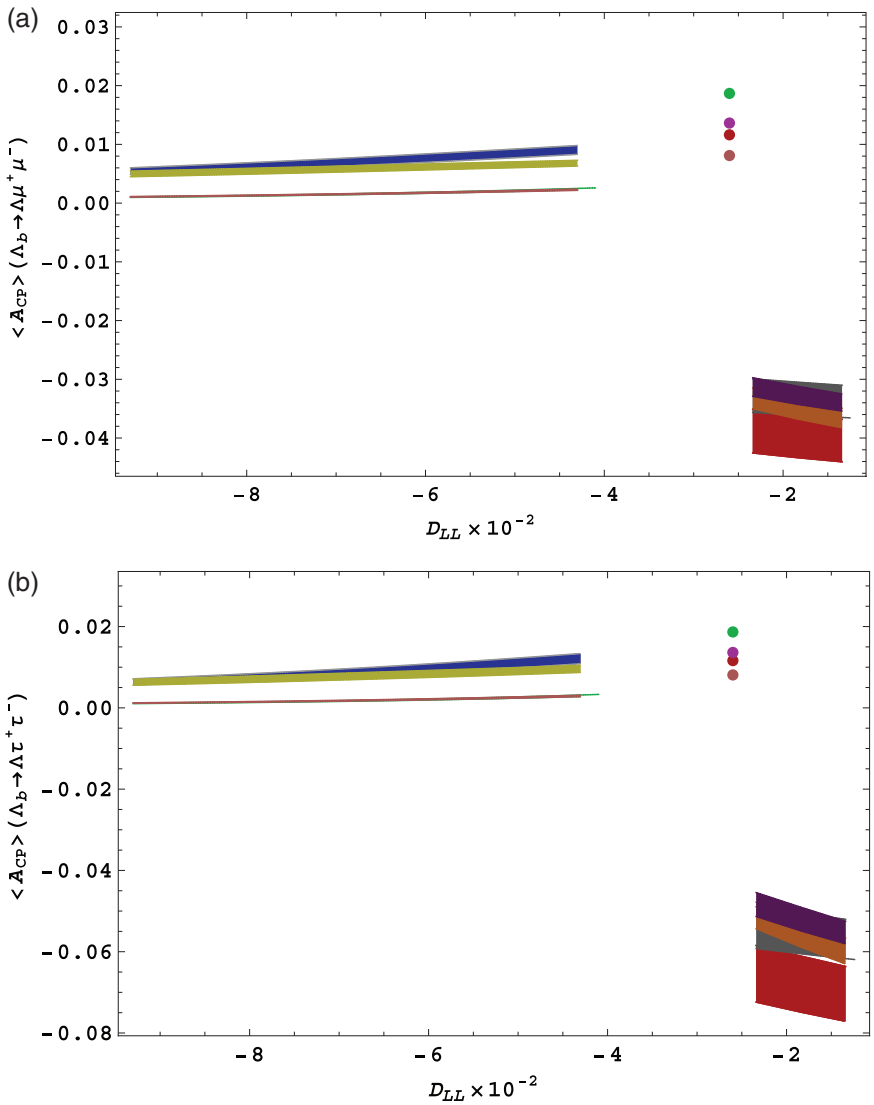

Fig. 1. Unpolarized CP-violation asymmetry $\mathcal{A}_{\rm CP}$ as a function of D_{LL} for $\Lambda_b \to \Lambda \mu^+ \mu^- (\tau^+ \tau^-)$ for scenarios $\mathcal{S}1$, $\mathcal{S}2$, and $\mathcal{S}3$. The red, blue, gray, and yellow bands correspond to $\mathcal{S}1$. The green, orange, pink, and purple bands correspond to $\mathcal{S}2$. The dots of different colors correspond to $\mathcal{S}3$. The band in each case depicts the variations of ϕ_{sb} in the respective scenario.

the coupling parameters of the Z' model are collected in Table 5, where $\mathcal{S}1$ and $\mathcal{S}2$ correspond to two different fitting values for B_s–$\bar{B}_s$ mixing data from the UTfit Collaboration [38–44].

Motivated by the latest results on the CP-violating phase ϕ_S^L and the like-sign dimuon charge asymmetry A_{SL}^b of the semileptonic decays given in Refs. [92–96], a detailed study has been performed by Li et al. [91]. The main emphasis of the study is to check if a simultaneous explanation for all mixing

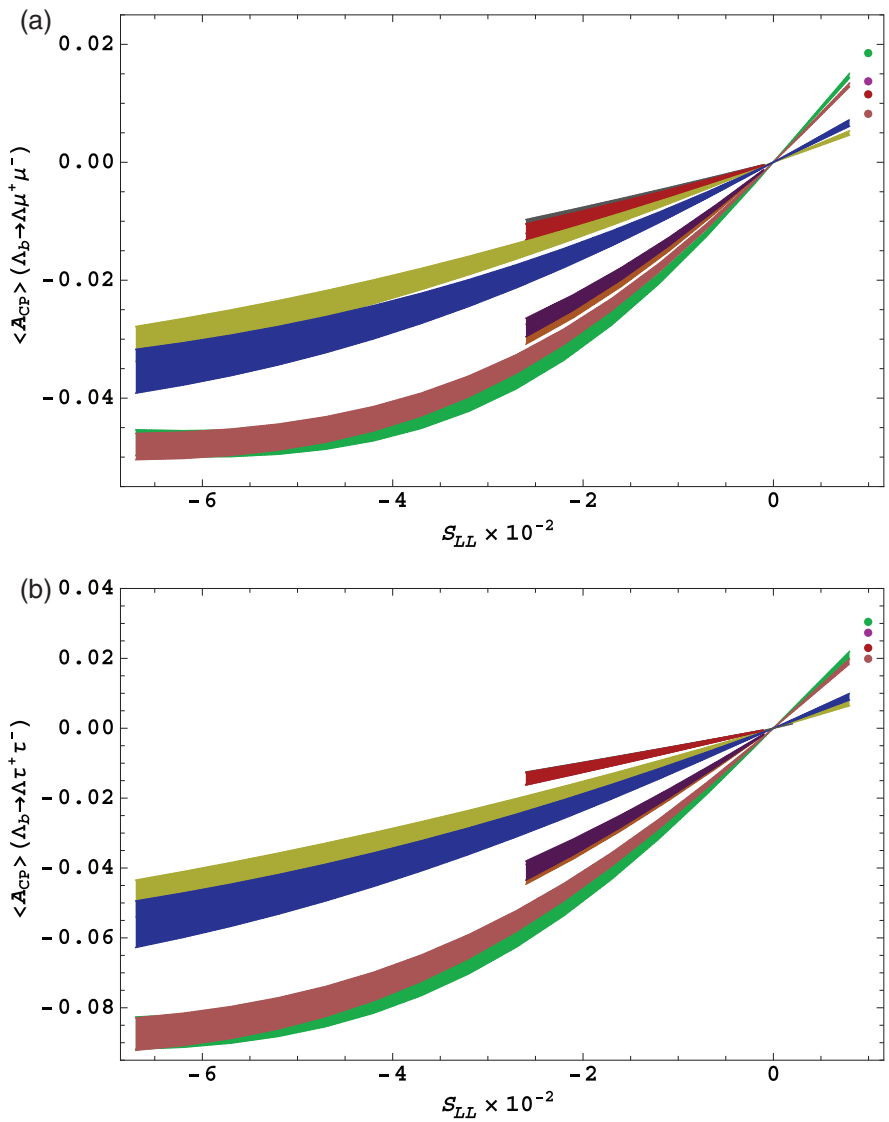

Fig. 2. Unpolarized CP-violation asymmetry $\mathcal{A}_{\rm CP}$ as a function of S_{LL} for $\Lambda_b \to \Lambda\mu^+\mu^-(\tau^+\tau^-)$ for scenarios $\mathcal{S}1$, $\mathcal{S}2$, and $\mathcal{S}3$. The color and band description is the same as in Fig. 1.

observables, especially the like-sign dimuon asymmetry A^b_{SL}, could be found for the Z' model. It has been found that it is not possible to accommodate all the data simultaneously and the new constraints on the CP-violating phase ϕ_S and $|\mathcal{B}_{sb}|$ are obtained from ΔM_S, ϕ_S, $\Delta\Gamma_S$ data. In addition, the constraints on $S^L_{\ell\ell}$ and $S^R_{\ell\ell}$ are obtained from the analysis of $B \to X_s\mu^+\mu^-$ [97], $B \to K^*\mu^+\mu^-$ [98,99], and $B \to \mu^+\mu^-$ [100]. In this paper, this is called scenario $\mathcal{S}3$. The corresponding numerical values are chosen from Refs. [97,101] and are summarized in Table 5.

It has already been mentioned that $\mathcal{B}_{sb} = |\mathcal{B}_{sb}|e^{-i\phi_{sb}}$ is the off-diagonal left-handed coupling of the Z' boson with quarks and ϕ_{sb} corresponds to a new weak phase, whereas S_{LL} and D_{LL} represent the combination of left- and right-handed couplings of Z' with the leptons (c.f. Eq. (8)). In addition to this weak phase, there is also an SM strong phase that has already been incorporated into the Wilson coefficient C_9. In order to fully scan the three scenarios, let us make a remark that using $D_{LL} \neq 0$ depicts the situation when the new physics comes only from the modification in the Wilson coefficient C_{10}, while the opposite case, $S_{LL} \neq 0$, indicates that the new physics is due to the change

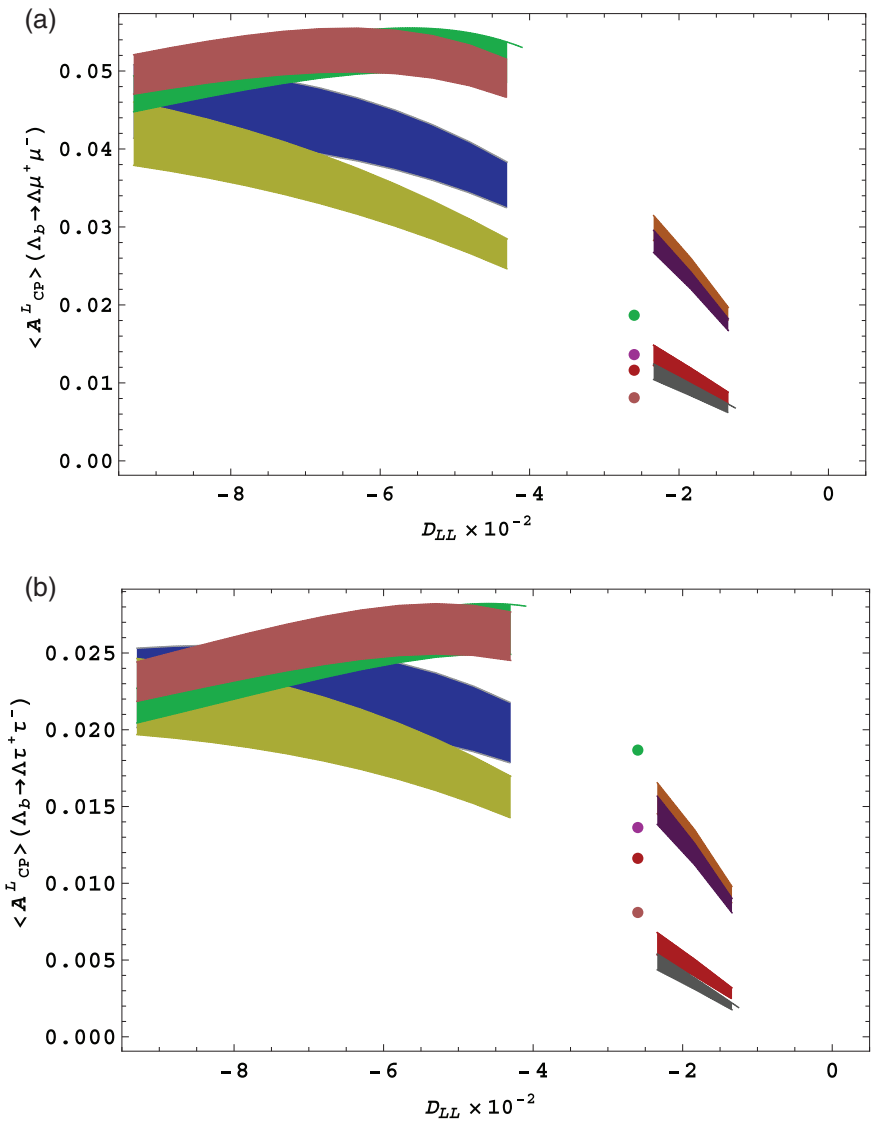

Fig. 3. Longitudinally polarized CP-violation asymmetry $\mathcal{A}^{L}_{\rm CP}$ as a function of D_{LL} for $\Lambda_b \to \Lambda\mu^+\mu^-(\tau^+\tau^-)$ for scenarios $\mathcal{S}1$, $\mathcal{S}2$, and $\mathcal{S}3$. The color and band description is the same as in Fig. 1.

in the Wilson coefficient C_9 (see Eq. (8)). In Figs. 1 to 8 the average CP-violating asymmetries, after integration on s, as a function of S_{LL} and D_{LL} are depicted. The different color codes along with the values of the Z' parameters in scenarios $\mathcal{S}1$ and $\mathcal{S}2$ are summarized in Table 6. However, for scenario $\mathcal{S}3$, the values of the Z' parameters with different color codes are given in Eq. (53) below:

$$\begin{aligned} |\mathcal{B}_{sb}| = 3 \times 10^{-3} : \begin{cases} \phi_{sb} = -140^\circ, \text{ magenta dot} \\ \phi_{sb} = -160^\circ, \text{ pink dot} \end{cases}; \\ |\mathcal{B}_{sb}| = 5 \times 10^{-3} : \begin{cases} \phi_{sb} = -140^\circ, \text{ green dot} \\ \phi_{sb} = -160^\circ, \text{ red dot} \end{cases}. \end{aligned} \tag{53}$$

Unpolarized CP-violation asymmetry:

- Figures 1 and 2 represent the unpolarized CP-violation asymmetries for the decay $\Lambda_b \to \Lambda\mu^+\mu^-(\tau^+\tau^-)$ as a function of D_{LL} and S_{LL}, respectively. In SM the CP-violation

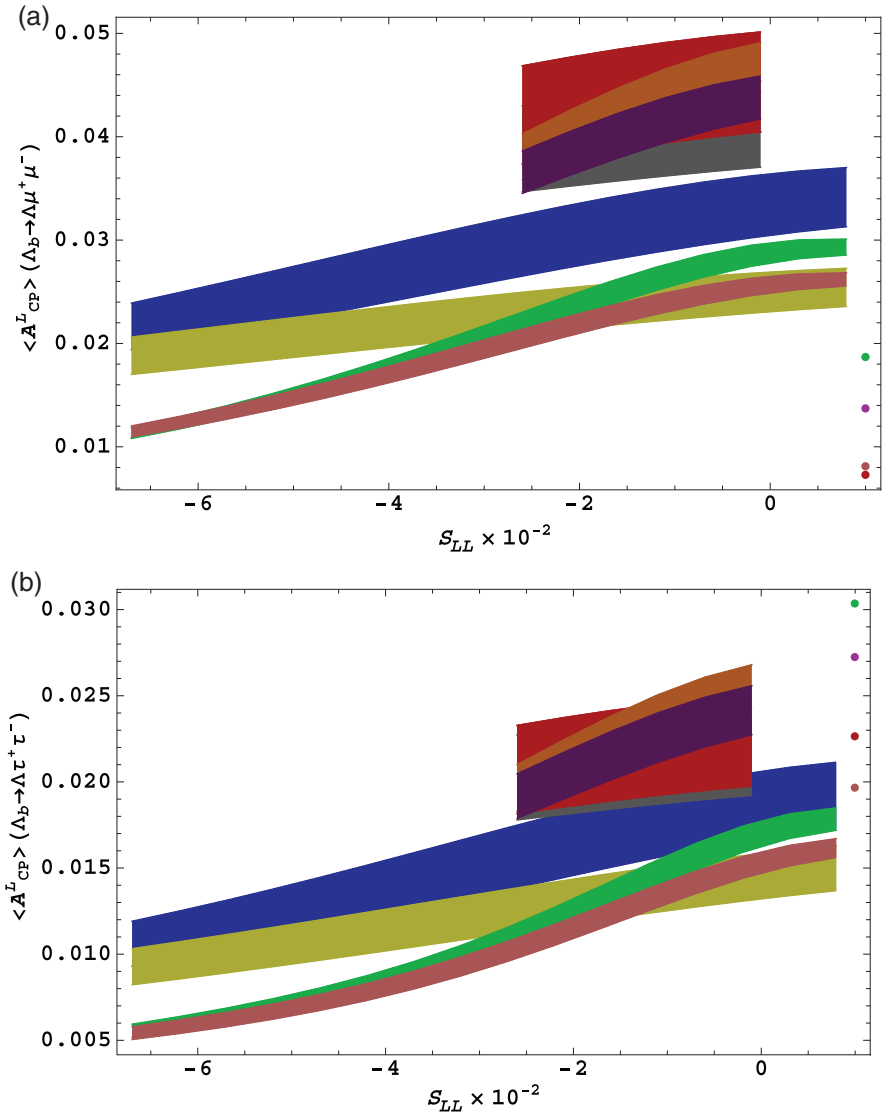

Fig. 4. Longitudinal polarized CP-violation asymmetry $\mathcal{A}^L_{\rm CP}$ as a function of S_{LL} for $\Lambda_b \to \Lambda\mu^+\mu^-(\tau^+\tau^-)$ for scenarios $\mathcal{S}1$, $\mathcal{S}2$, and $\mathcal{S}3$. The color and band description is the same as in Fig. 1.

asymmetry is zero, hence a non-zero value will give us a clue to physics beyond the Standard Model, which is commonly known as New Physics (NP). It is evident from Eq. (24) that $\mathcal{A}_{\rm CP}$ is proportional to the Z' parameters that come through the imaginary part of the Wilson coefficients as well as to the weak phase ϕ_{sb}, which is concealed in Λ_{sb} (c.f. Eq. (7)). Therefore, dependence on the new weak phase ϕ_{sb} is expected, and this is evident from Figs. 1 and 2, where the band in each case depicts the variations of the phase ϕ_{sb} in the respective scenarios. In Fig. 1, $\mathcal{A}_{\rm CP}$ is plotted with D_{LL} by changing the values of S_{LL}, ϕ_{sb}, and B_{sb}. In the case of μ as final-state leptons, the value of $\mathcal{A}_{\rm CP}$ is positive in both scenarios $\mathcal{S}1$ and $\mathcal{S}2$ but for positive values of S_{LL}. However, the value of $\mathcal{A}_{\rm CP}$ reaches around -0.045 when $D_{LL} = -1.6 \times 10^{-2}$ and the corresponding $S_{LL} = -6.7 \times 10^{-2}$, depicted by the lowest end ($\phi_{sb} = -65^\circ$) of the red band. Similarly, for the case of τ as final-state leptons, the value of $\mathcal{A}_{\rm CP}$ is positive in both scenarios for positive values of S_{LL}. However, the value of $\mathcal{A}_{\rm CP}$ is around -0.08 for $D_{LL} = -1.6 \times 10^{-2}$ and $S_{LL} = -6.7 \times 10^{-2}$, shown by the bottom line of the red band.

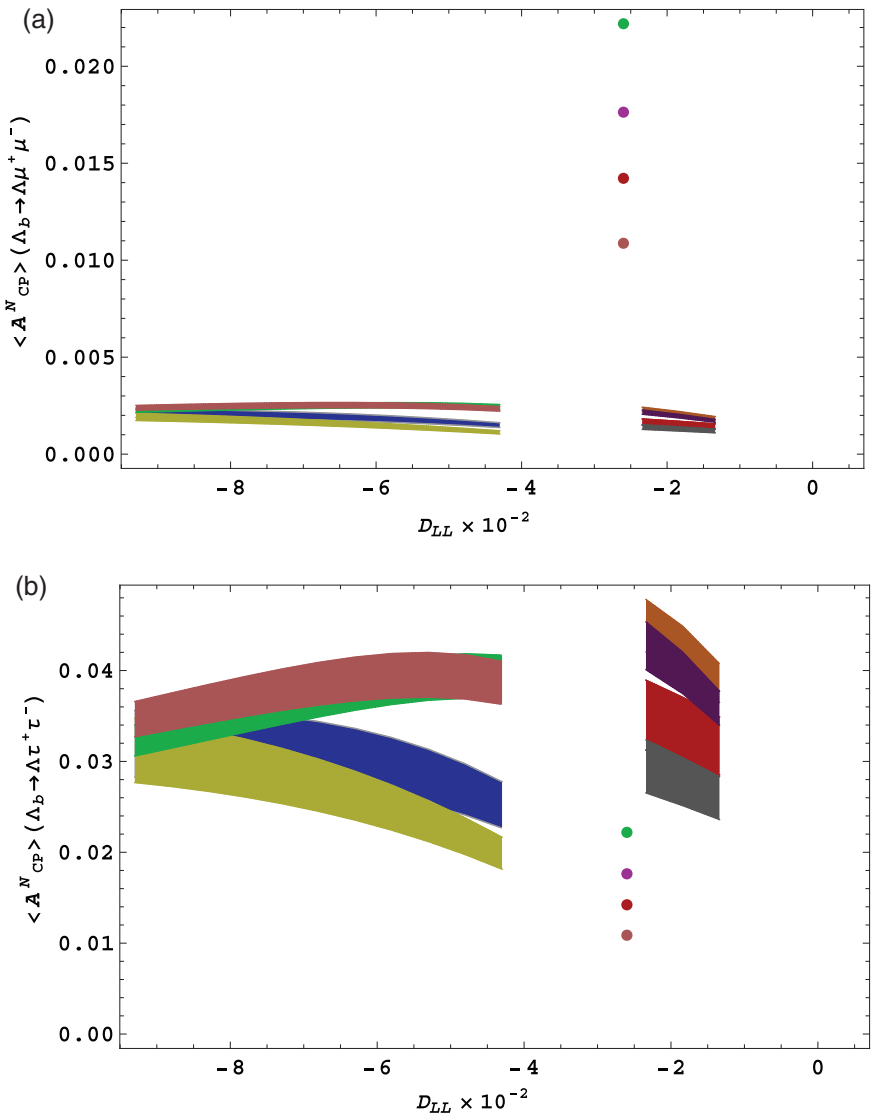

Fig. 5. Normal polarized CP-violation asymmetry $\mathcal{A}^N_{\rm CP}$ as a function of D_{LL} for $\Lambda_b \to \Lambda\mu^+\mu^-(\tau^+\tau^-)$ for scenarios $\mathcal{S}1$, $\mathcal{S}2$, and $\mathcal{S}3$. The color and band description is the same as in Fig. 1.

- Figure 2 presents the behavior of $\mathcal{A}_{\rm CP}$ with S_{LL} by varying the values of D_{LL}, ϕ_{sb}, and $\mathcal{B}_{sb}$ in the range given in Table 5. It can be immediately noticed that, in the μ case, the value is small compared to the case when τ are final-state leptons. In both cases, $\mathcal{A}_{\rm CP}$ is an increasing function of S_{LL}. In $\Lambda_b \to \Lambda\tau^+\tau^-$, the value of unpolarized CP asymmetry is around -0.1 when $S_{LL} = -6.7 \times 10^{-2}$.

  The values of unpolarized CP-violation asymmetries in scenario $\mathcal{S}3$ for $\Lambda_b \to \Lambda\mu^+\mu^-$ and $\Lambda_b \to \Lambda\tau^+\tau^-$ are shown by different color dots in Figs. 1(b) and 2(b). It can be noticed that the value of unpolarized CP-violation asymmetry is positive maximum in this scenario when $\phi_{sb} = -140^\circ$, $|\mathcal{B}_{sb}| = 5 \times 10^{-3}$; it is shown by the green dot in these figures. Irrespective of the negative or positive values of the new weak phase (ϕ_{sb}), the value of CP asymmetry remains positive for all values of $\mathcal{B}_{sb}$, which is an entirely distinctive feature compared to the first two scenarios, where the CP asymmetries climb from negative to positive values.

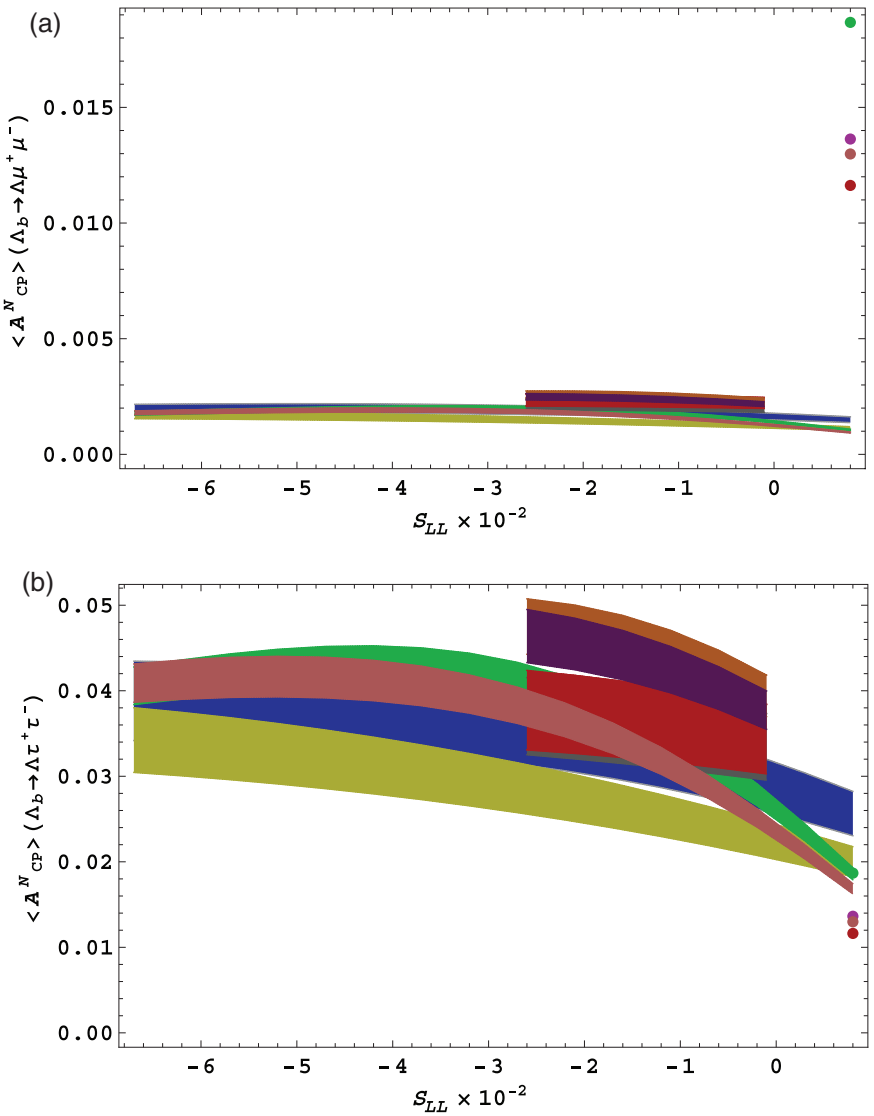

Fig. 6. Normal polarized CP-violation asymmetry $\mathcal{A}_{\rm CP}^{N}$ as a function of S_{LL} for $\Lambda_b \to \Lambda\mu^+\mu^-(\tau^+\tau^-)$ for scenarios $\mathcal{S}1$, $\mathcal{S}2$, and $\mathcal{S}3$. The color and band description is the same as in Fig. 1.

Longitudinal polarized CP-violation asymmetry:

- The longitudinal polarized CP-violation asymmetry $\mathcal{A}_{\rm CP}^{L}$ is plotted in Figs. 3 and 4. From Eq. (31) it can be noticed that $\mathcal{Q}^{L}$ is proportional to the imaginary part of the combination of Wilson coefficients that involve C_7, C_9, and C_{10} in both the SM as well as the Z' model. This occurs even though the Wilson coefficient C_7 does not get a contribution from Z'; the change in the Wilson coefficients C_9 and C_{10} due to the parameters of the Z' model will make $\mathcal{A}_{\rm CP}^{L}$ sensitive to the change arising due to an extra neutral boson Z'. In Figs. 3(a) and (b), we have plotted $\mathcal{A}_{\rm CP}^{L}$ vs D_{LL} by fixing the values of S_{LL} and other Z' parameters in the range given in Table 5. We can see that the value of $\mathcal{A}_{\rm CP}^{L}$ increases from 0.008 to 0.053 when μ are the final-state leptons and from 0.004 to 0.030 in the case of τ as final-state leptons, which can be visualized from the color bands that correspond to scenario $\mathcal{S}1$ ($\mathcal{S}2$). The situation when the longitudinal polarized CP-violation asymmetry is plotted with S_{LL} by taking other parameters in the range given in Table 5 is displayed in Fig. 4. Here we can see that it is an increasing function of S_{LL}, where in

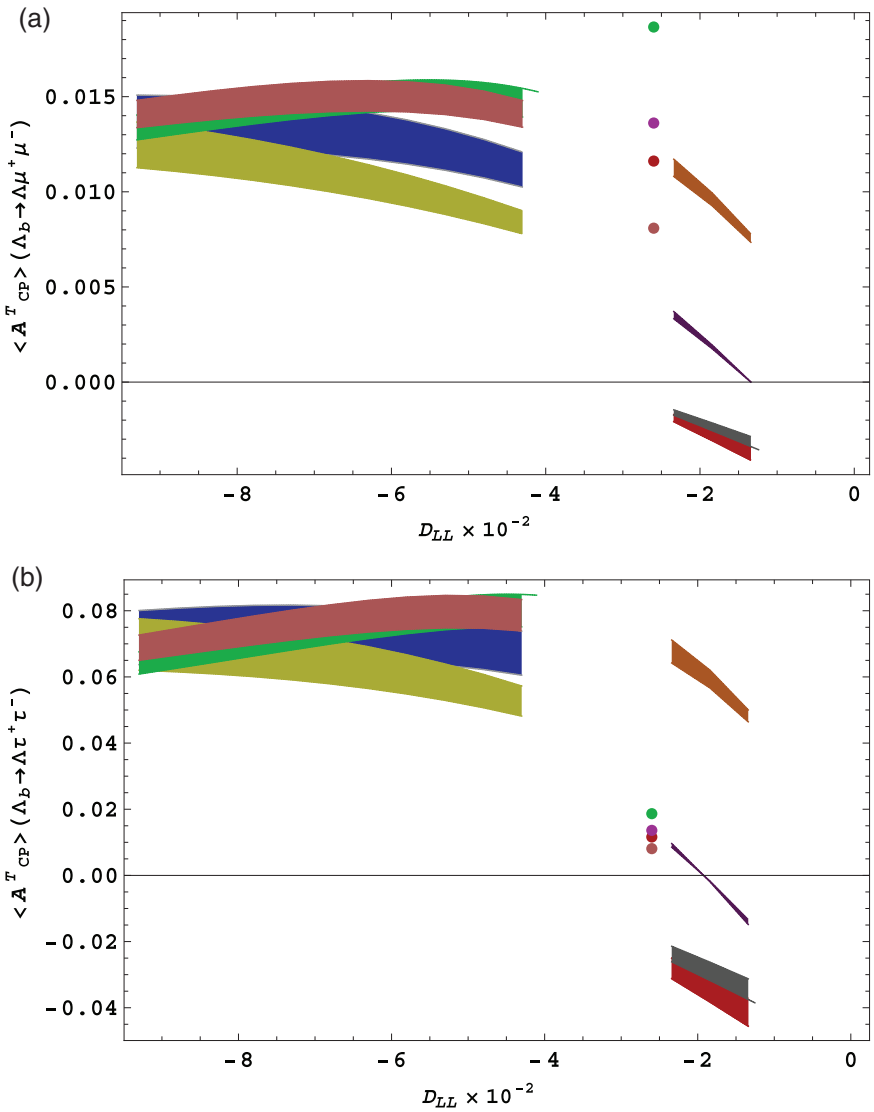

Fig. 7. Transverse polarized CP-violation asymmetry $\mathcal{A}^T_{\rm CP}$ as a function of D_{LL} for $\Lambda_b \to \Lambda\mu^+\mu^-(\tau^+\tau^-)$ for scenarios $\mathcal{S}1$, $\mathcal{S}2$, and $\mathcal{S}3$. The color and band description is the same as in Fig. 1.

$\mathcal{S}1$ and $\mathcal{S}2$ the values increase from 0.01 (0.005) to 0.05 (0.025) when we have μ (τ) as final-state leptons; this is clearly visible from the red (pink) band. It can also be seen in Figs. 3(a) and 4(a) that the value of the longitudinal polarized CP-violation asymmetry in scenario $\mathcal{S}3$ is much suppressed when we have μ as final-state leptons. However, in the τ case, the value of the longitudinal CP-violation asymmetry is around 0.030 when $\phi_{sb} = -140^\circ$ and $|\mathcal{B}_{sb}| = 5 \times 10^{-3}$. This is shown with the green dot in Figs. 3(b) and 4(b). It can be noticed that the value of longitudinal polarized CP-violation asymmetry in $\Lambda_b \to \Lambda\tau^+\tau^-$ is significantly different from its value in $\mathcal{S}1$ and $\mathcal{S}2$. Hence, by measuring $\mathcal{A}^L_{\rm CP}$, one can not only segregate the NP coming through the Z' boson but can also distinguish the three scenarios.

Normal polarized CP-violation asymmetry:

- In contrast to $\mathcal{A}_{\rm CP}$ and $\mathcal{A}^L_{\rm CP}$, the normal polarized CP-violation asymmetry ($\mathcal{A}^N_{\rm CP}$) is an order of magnitude smaller in the μ case compared to the case of τ as final-state leptons. By looking at Eq. (35), $\mathcal{A}^N_{\rm CP}$ comes from the function $\mathcal{Q}^N$, which contains $\mathcal{H}_1, \ldots, \mathcal{H}_6$. In Eqs. (36)–(40)

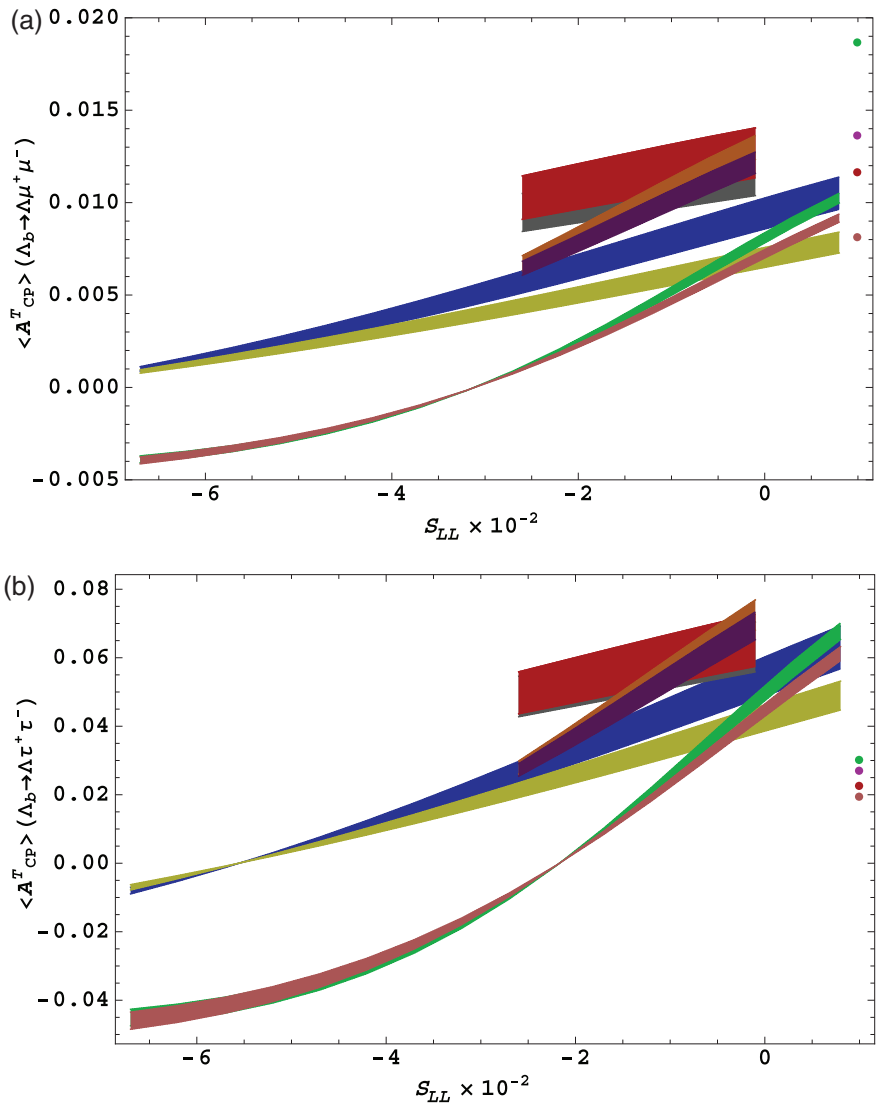

Fig. 8. Transverse polarized CP-violation asymmetry $\mathcal{A}^T_{\rm CP}$ as a function of S_{LL} for $\Lambda_b \to \Lambda\mu^+\mu^-(\tau^+\tau^-)$ for scenarios $\mathcal{S}1$, $\mathcal{S}2$, and $\mathcal{S}3$. The color and band description is the same as in Fig. 1.

it is clear that these asymmetries are proportional to the lepton mass and their suppression in the muon case is obvious; Figs. 5(a) and 6(a) depict this fact. Coming to Figs. 5(b) and 6(b) we can see that $\mathcal{A}^N_{\rm CP}$ is very sensitive to the parameters of Z' both in $\mathcal{S}1$ and $\mathcal{S}2$. In Fig. 5(b), the value of $\mathcal{A}^N_{\rm CP}$ decreases from 0.040 to 0.018 in the parameter range of Z' in $\mathcal{S}1$ and from 0.048 to 0.028 in $\mathcal{S}2$. The situation remains the same as in Fig. 5 when $\mathcal{A}^N_{\rm CP}$ is plotted with S_{LL} in Figs. 6(a) and 6(b). It can also be noted that the average value of $\mathcal{A}^N_{\rm CP}$ increases from 0.020 to 0.045 in $\mathcal{S}1$ and 0.035 to 0.05 in $\mathcal{S}2$.

What turns out to be more interesting is the impact of parametric space on scenario $\mathcal{S}3$ in the case of μ and final-state leptons. In this scenario, the value of the normal CP-violation asymmetry in $\Lambda_b \to \Lambda\mu^+\mu^-$ is an order of magnitude larger than the corresponding values in $\mathcal{S}1$ and $\mathcal{S}2$. Here, the maximum value is 0.018 (the green dot) when $\phi_{sb} = -140^\circ$ and $\left|\mathcal{B}_{sb}\right| = 5 \times 10^{-3}$ while, in the case of τ as final-state leptons, the order of asymmetries remains the same as in $\mathcal{S}1$ and $\mathcal{S}2$.

Table 6. Color bands for Figs. 1–8 $\langle \mathcal{A}_{\rm CP} \rangle$ and $\langle \mathcal{A}^i_{\rm CP} \rangle$ vs S_{LL} and D_{LL} for scenarios $\mathcal{S}1$ and $\mathcal{S}2$.

Color region	ϕ_{sb}	$\lvert\mathcal{B}_{sb}\rvert \times 10^{-3}$	$\langle \mathcal{A}_{\rm CP} \rangle$ and $\langle \mathcal{A}^i_{\rm CP} \rangle$ vs S_{LL} $D_{LL} \times 10^{-2}$	$\langle \mathcal{A}_{\rm CP} \rangle$ and $\langle \mathcal{A}^i_{\rm CP} \rangle$ vs D_{LL} $S_{LL} \times 10^{-2}$
	-79°			
Blue		1.31	-4.1	1.1
	-65°			
	-79°			
Red		1.31	-9.3	-6.7
	-65°			
	-79°			
Yellow		0.87	-4.1	1.1
	-65°			
	-79°			
Gray		0.87	-9.3	-6.7
	-65°			
	-86°			
Green		2.35	-1.6	0.2
	-78°			
	-86°			
Orange		2.35	-3.4	-2.6
	-78°			
	-86°			
Pink		2.05	-1.6	0.2
	-78°			
	-86°			
Purple		2.05	-3.4	-2.6
	-78°			

Transverse polarized CP-violation asymmetry:

- Just like the normal polarized CP-violation asymmetry, the different terms in transverse polarized CP-violation asymmetry $\mathcal{A}^T_{\rm CP}$ are also m_l-suppressed, which is visible from $\mathcal{H}$ appearing in the function $\mathcal{Q}^T$ in Eq. (42). The graphs in Figs. 7(a) and 8(a) depict the fact that, in the presence of NP coming through the Z' boson, the maximum value of $\mathcal{A}^T_{\rm CP}$ is around 0.016 (shown by the green band) in $\Lambda_b \to \Lambda\mu^+\mu^-$, while Figs. 7(b) and 8(b) show that, in the case of τ as final-state leptons, the value of $\mathcal{A}^T_{\rm CP}$ reaches up to 0.08 in a certain parametric space of the Z' scenario $\mathcal{S}1$.

  By varying the Z' parameters in the range given in Eq. (53), the trend of transverse CP-violation asymmetry is shown by different colors of dots in Fig. 8. In the case of μ as final-state leptons, we can see that, for $\phi_{sb} = -140^\circ$, $|\mathcal{B}_{sb}| = 5 \times 10^{-3}$, in scenario $\mathcal{S}3$ the value of transverse polarized CP-violation asymmetry is slightly higher than the first two scenarios (shown by the green dot). However, in $\Lambda_b \to \Lambda\tau^+\tau^-$ decay the effects coming through the parametric space of $\mathcal{S}3$ are smaller than that of the first two scenarios.

In short, we have analyzed the imprints of NP coming through the neutral Z' boson on the unpolarized and polarized CP-violation asymmetries in $\Lambda_b \to \Lambda\ell^+\ell^-$ decays. In addition, motivated by the fact that the CP-violation asymmetry is negligible in the SM, we have chosen this observable to explore the effects of Z' in $\Lambda_b \to \Lambda\ell^+\ell^-$ decays. It has been noticed that the values of unpolarized and polarized CP-violation asymmetries are considerable in both the $\Lambda_b \to \Lambda\mu^+\mu^-$ and $\Lambda_b \to \Lambda\tau^+\tau^-$ channels and hence this gives a clear message of NP arising from the neutral Z' boson. Though the

detection of lepton polarization effects in semileptonic decays is really a daunting task at experiments such as ATLAS and CMS and at LHCb, these CP-violation asymmetries, which suffer less from hadronic uncertainties, provide a useful probe to establish the NP coming through the Z' model.

Acknowledgements

M.J.A. would like to thank Quaid-i-Azam University for the support given through the University Research Fund. M.A.P. and I.A. would like to acknowledge the grants (2012/13047-2) and (2013/23177-3) from FAPESP. The authors would like to thank Bruno El-Bennich for useful discussions.

Funding

Open Access funding: SCOAP[3].

References

[1] S. L. Glashow, J. Iliopoulos, and L. Maiani, Phys. Rev. D **2**, 1285 (1970).
[2] W. Altmannshofer, P. Ball, A. Bharucha, A. Buras, D. Straub, and M. Wick, J. High Energy Phys. **0901**, 019 (2009).
[3] U. Egede et al., J. High Energy Phys. **1010**, 056 (2010).
[4] A. Ishikawa et al. [Belle Collaboration], Phys. Rev. Lett. **91**, 261601 (2003).
[5] B. Aubert et al. [BaBar Collaboration], Phys. Rev. D **73**, 092001 (2006).
[6] A. Ali, P. Ball, L. T. Handoko, and G. Hiller, Phys. Rev. D **61**, 074024 (2000).
[7] T. M. Aliev, C. S. Kim, and Y. G. Kim, Phys. Rev. D **62**, 014026 (2000).
[8] T. M. Aliev, D. A. Demir, and M. Savci, Phys. Rev. D **62**, 074016 (2000).
[9] M. A. Paracha, I. Ahmed, and M. J. Aslam, Eur. Phys. J. C **52**, 967 (2007).
[10] I. Ahmed, M. A. Paracha, and M. J. Aslam, Eur. Phys. J. C **54**, 591 (2008).
[11] A. Saddique, M. J. Aslam, and C. D. Lu, Eur. Phys. J. C **56**, 267 (2008).
[12] I. Ahmed, M. Jamil Aslam, and M. Ali Paracha, Phys. Rev. D **89**, 015006 (2014).
[13] M. Jamil Aslam, Y.-M. Wang, and C.-D. Lu, Phys. Rev. D **78**, 114032 (2008).
[14] Y.-M. Wang, M. Jamil Aslam, and C.-D. Lu, Eur. Phys. J. C **59**, 847 (2009).
[15] T. M. Aliev and M. Savci, Nucl. Phys. B **863**, 398 (2012).
[16] T. M. Aliev and M. Savci, Phys. Lett. B **718**, 566 (2012).
[17] F. Gursey and M. Serdaroglu, Lett. Nuovo Cimento **21**, 28 (1978).
[18] G. Buchalla, G. Burdman, C. T. Hill, and D. Kominis, Phys. Rev. D **53**, 5185 (1996) [arXiv:9510376 [hep-ph]] [Search INSPIRE].
[19] E. Nardi, Phys. Rev. D **48**, 1240 (1993).
[20] J. Bernabeu, E. Nardi, and D. Tommasini, Nucl. Phys. B **409**, 69 (1993) [arXiv:930625 [hep-ph]] [Search INSPIRE].
[21] V. Barger, M. Berger, and R. J. Phillips, Phys. Rev. D **52**, 1663 (1995).
[22] E. Eichten, I. Hinchliffe, K. D. Lane, and C. Quigg, Rev. Mod. Phys. **56**, 579 (1984).
[23] P. Langacker and M. Plümacher, Phys. Rev. D **62**, 013006 (2000).
[24] J. L. Lopez and D. V. Nanopoulos, Phys. Rev. D **55**, 397 (1997).
[25] B. B. Sirvanli, Mod. Phys. Lett. A **23**, 347 (2008).
[26] M. S. Carena, A. Daleo, B. A. Dobrescu, and T. M. P. Tait, Phys. Rev. D **70**, 093009 (2004) [arXiv:0408098 [hep-ph]] [Search INSPIRE].
[27] T. G. Rizzo, [arXiv:0610104 [hep-ph]] [Search INSPIRE].
[28] T. G. Rizzo, [arXiv:0808.1506 [hep-ph]].
[29] A. Abulencia et al. [CDF Collaboration], Phys. Rev. Lett. **96**, 211801 (2006) [arXiv:0602045 [hep-ex]] [Search INSPIRE].
[30] V. Barger, L. Everett, J. Jiang, P. Langacker, T. Liu, and C. Wagner, Phys. Rev. D **80**, 055008 (2009) [arXiv:0902.4507 [hep-ph]] [Search INSPIRE].
[31] V. Barger, L. L. Everett, J. Jiang, P. Langacker, T. Liu, and C. E. M. Wagner, J. High Energy Phys. **0912**, 048 (2009) [arXiv:0906.3745 [hep-ph]] [Search INSPIRE].
[32] Q. Chang, X. Q. Li, and Y. D. Yang, J. High Energy Phys. **1002**, 082 (2010) [arXiv:0907.4408 [hep-ph]] [Search INSPIRE].

[33] V. Barger, C.-W. Chiang, J. Jiang, and P. Langacker, Phys. Lett. B **596**, 229 (2004) [arXiv:0405108 [hep-ph]] [Search INSPIRE].
[34] K. Cheung, C.-W. Chiang, N. G. Deshpande, and J. Jiang, Phys. Lett. B **652**, 285 (2007) [arXiv:0604223 [hep-ph]] [Search INSPIRE].
[35] X.-G. He and G. Valencia, Phys. Rev. D **74**, 013011 (2006) [arXiv:0605202 [hep-ph]] [Search INSPIRE].
[36] S. Baek, J. H. Jeon, and C. S. Kim, Phys. Lett. B **664**, 84 (2008) [arXiv:0803.0062 [hep-ph]] [Search INSPIRE].
[37] S. Sahoo, C. K. Das, and L. Maharana, Int. J. Mod. Phys. A **26**, 3347 (2011) [arXiv:1112.0460 [hep-ph]] [Search INSPIRE].
[38] M. Bona et al. [UTfit Collaboration], PMC Phys. A **3**, 6 (2009) [arXiv:0803.0659 [hep-ph]] [Search INSPIRE].
[39] M. Bona et al., [arXiv:0906.0953 [hep-ph]] [Search INSPIRE].
[40] C.-H. Chen, Phys. Lett. B **683**, 160 (2010) [arXiv:0911.3479 [hep-ph]] [Search INSPIRE].
[41] N. G. Deshpande, X.-G. He, and G. Valencia, Phys. Rev. D **82**, 056013 (2010) [arXiv:1006.1682 [hep-ph]] [Search INSPIRE].
[42] J. E. Kim, M.-S. Seo, and S. Shin, Phys. Rev. D **83**, 036003 (2011) [arXiv:1010.5123 [hep-ph]] [Search INSPIRE].
[43] P. J. Fox, J. Liu, D. Tucker-Smith, and N. Weiner, Phys. Rev. D **84**, 115006 (2011) [arXiv:1104.4127 [hep-ph]] [Search INSPIRE].
[44] Q. Chang, R.-M. Wang, Y.-G. Xu, and X.-W. Cui, Chinese Phys. Lett. **28**, 081301 (2011).
[45] C. Bobeth and U. Haisch, [arXiv:1109.1826 [hep-ph]] [Search INSPIRE].
[46] A. K. Alok, S. Baek, and D. London, J. High Energy Phys. **1107**, 111 (2011) [arXiv:1010.1333 [hep-ph]] [Search INSPIRE].
[47] X.-Q. Li, Y.-M. Li, G.-R. Lu, and F. Su, [arXiv:1204.5250 [hep-ph]] [Search INSPIRE].
[48] V. Barger, C.-W. Chiang, P. Langacker, and H.-S. Lee, Phys. Lett. B **580**, 186 (2004) [arXiv:0310073 [hep-ph]] [Search INSPIRE].
[49] C.-W. Chiang, R.-H. Li, and C.-D. Lu, [arXiv:0911.2399 [hep-ph]] [Search INSPIRE].
[50] J. Hua, C. S. Kim, and Y. Li, Eur. Phys. J. C **69**, 139 (2010) [arXiv:1002.2531 [hep-ph]] [Search INSPIRE].
[51] Q. Chang, X.-Q. Li, and Y.-D. Yang, J. High Energy Phys. **1004**, 052 (2010) [arXiv:1002.2758 [hep-ph]] [Search INSPIRE].
[52] Q. Chang and Y.-H. Gao, Nucl. Phys. B **845**, 179 (2011) [arXiv:1101.1272 [hep-ph]] [Search INSPIRE].
[53] Y. Li, J. Hua, and K.-C. Yang, Eur. Phys. J. C **71**, 1775 (2011) [arXiv:1107.0630 [hep-ph]] [Search INSPIRE].
[54] C.-W. Chiang, Y.-F. Lin, and J. Tandean, J. High Energy Phys. **1111**, 083 (2011) [arXiv:1108.3969 [hep-ph]] [Search INSPIRE].
[55] S. Sahoo, C. K. Das, and L. Maharana, Int. J. Mod. Phys. A **24**, 6223 (2009) [arXiv:1112.4563 [hep-ph]].
[56] N. Katrici and T. M. Aliev, [arXiv:1207.4053 [hep-ph]] [Search INSPIRE].
[57] V. Barger, C.-W. Chiang, P. Langacker, and H.-S. Lee, Phys. Lett. B **598**, 218 (2004) [arXiv:0406126 [hep-ph]] [Search INSPIRE].
[58] R. Mohanta and A. K. Giri, Phys. Rev. D **79**, 057902 (2009) [arXiv:0812.1842 [hep-ph]] [Search INSPIRE].
[59] Q. Chang, X.-Q. Li, and Y.-D. Yang, J. High Energy Phys. **0905**, 056 (2009) [arXiv:0903.0275 [hep-ph]] [Search INSPIRE].
[60] J. Hua, C. S. Kim, and Y. Li, Phys. Lett. B **690**, (2010) 508 [arXiv:1002.2532 [hep-ph]] [Search INSPIRE].
[61] Q. Chang, X.-Q. Li, and Y.-D. Yang, Int. J. Mod. Phys. A **26**, 1273 (2011) [arXiv:1003.6051 [hep-ph]] [Search INSPIRE].
[62] Q. Chang and Y.-D. Yang, Nucl. Phys. B **852**, 539 (2011) [arXiv:1010.3181 [hep-ph]] [Search INSPIRE].
[63] L. Hofer, D. Scherer, and L. Vernazza, J. High Energy Phys. **1102**, 080 (2011) [arXiv:1011.6319 [hep-ph]] [Search INSPIRE].
[64] Y. Li, X.-J. Fan, J. Hua, and E.-L. Wang, [arXiv:1111.7153 [hep-ph]] [Search INSPIRE].

[65] S. Sahoo, C. K. Das, and L. Maharana, Phys. Atom. Nucl. **74**, 1032 (2011) [arXiv:1112.2246 [hep-ph]] [Search INSPIRE].
[66] S. Sahoo and L. Maharana, Indian J. Pure Appl. Phys. **46**, 306 (2008).
[67] I. Ahmed, Phys. Rev. D **86**, 095022 (2012).
[68] T. Mannel and S. Recksiegel, J. Phys. G **24**, 979 (1998).
[69] T. Aaltonen et al., Phys. Rev. Lett. **107**, 201802 (2011).
[70] R. Aaij et al., Phys. Lett. B. **725**, 25 (2013).
[71] G. Buchalla, A. J. Buras, and M. E. Lautenbacher, Rev. Mod. Phys. **68**, 1125 (1996).
[72] A. J. Buras and M. Munz, Phys. Rev. D **52**, 186 (1995) [arXiv:9501281 [hep-ph]] [Search INSPIRE].
[73] A. J. Buras, M. Misiak, M. Munz, and S. Pokorski, Nucl. Phys. B **424**, 374 (1994).
[74] F. Kruger and L. M. Sehgal, Phys. Lett. B **380**, 199 (1996) [arXiv:9603237 [hep-ph]] [Search INSPIRE].
[75] B. Grinstein, M. J. Savag, and M. B. Wise, Nucl. Phys. B **319**, 271 (1989).
[76] G. Cella, G. Ricciardi, and A. Vicere, Phys. Lett. B **258**, 212 (1991).
[77] C. Bobeth, M. Misiak, and J. Urban, Nucl. Phys. B **574**, 291 (2000).
[78] H. H. Asatrian, H. M. Asatrian, C. Grueb, and M. Walker, Phys. Lett. B **507**, 162 (2001).
[79] M. Misiak, Nucl. Phys. B **393**, 23 (1993); **439**, 461 (1995) [erratum].
[80] T. Huber, T. Hurth, and E. Lunghi, [arXiv:0807.1940] [Search INSPIRE].
[81] Q. Chang and Y.-H. Gao, [arXiv:1101.1272v1 [hep-ph]].
[82] Y. Li and J. Hua, [arXiv:1107.0630v2 [hep-ph]].
[83] K. Cheung et al., Phys. Lett. B **652**, 285 (2007).
[84] C. H. Chen and H. Hatanaka, Phys. Rev. D **73**, 075003 (2006).
[85] C. W. Chiang et al., J. High Energy Phys. **0608**, 075 (2006).
[86] V. Barger et al., Phys. Lett. B **580**, 186 (2004).
[87] V. Barger et al., Phys. Rev. D **80**, 055008 (2009).
[88] R. Mohanta and A. K. Giri, Phys. Rev. D **79**, 057902 (2009).
[89] J. Hua, C. S. Kim, and Y. Li, Eur. Phys. J. C **69**, 139 (2010).
[90] T. M. Aliev, K. Azizi, and M. Savci, Phys. Rev. D **81**, 056006 (2010).
[91] X.-Q. Li, Y.-M. Li, and G.-R. Lin, J. High Energy Phys. **1205**, 049 (2012) [arXiv:1204.5250 [hep-ph]] [Search INSPIRE].
[92] V. Abazov et al. [D0 Collaboration], D0 conference note, 6098-CONF.
[93] T. Aaltonen et al. [CDF Collaboration], Phys. Rev. D **85**, 072002 (2012).
[94] R. Aaij et al. [LHCb Collaboration], Phys. Rev. Lett. **108**, 101803 (2012).
[95] R. Aaij et al. [LHCb Collaboration], Phys. Lett. B **707**, 497 (2012).
[96] V. Abazov et al. [CDF Collaboration], Phys. Rev. D **84**, 052007 (2011).
[97] M. Iwasaki et al. [Belle Collaboration], Phys. Rev. D **72**, 092005 (2005).
[98] J. P. Lees et al. [BaBar Collaboration], [arXiv:1204.3993 [hep-ex]].
[99] R. Aaij et al. [LHCb Collaboration], Phys. Rev. Lett. **108**, 181806 (2012).
[100] R. Aaij et al. [LHCb Collaboration], Phys. Rev. Lett. **108**, 231801 (2012).
[101] T. M. Aliev, K. Azizi, and M. Savci, Phys. Lett. B **718**, 566 (2012).